INVESTIGATIONS ON DISTRIBUTION STATIC COMPENSATOR WITH SOME CONTROL ALGORITHMS

DISSERTATION
SUBMITTED IN PARTIAL FULFILLMENT OF THE REQUIREMENTS
FOR THE AWARD OF THE DEGREE
OF

MASTER OF TECHNOLOGY
IN
POWER SYSTEM

Submitted by:

Sachin Kumar Kesharvani

Roll No. 2K12/PSY/20

Under the supervision of

DR. ALKA SINGH

DEPARTMENT OF ELECTRICAL ENGINEERING

DELHI TECHNOLOGICAL UNIVERSITY

(Formerly Delhi College of Engineering)

Bawana Road, Delhi-110042

2014

DEPARTMENT OF ELECTRICAL ENGINEERING

DELHI TECHNOLOGICAL UNIVERSITY

(Formerly Delhi College of Engineering)

Bawana Road, Delhi-110042

CERTIFICATE

I, **Sachin Kumar Kesharvani**, Roll No. 2K12/PSY/20 student of M.Tech (Power System), hereby declare that the dissertation/project titled **"Investigations on Distribution Static Compensator with some Control Algorithms"** under the supervision of **Dr. Alka Singh** of Electrical Department, Delhi Technological University in partial fulfillment of the requirement for the award of the degree of Master of Technology has not been submitted elsewhere for the award of any degree.

Place: Delhi **(SACHIN KUMAR KESHARVANI)**

Date: 31.07.2014

Dr. ALKA SINGH

(SUPERVISOR)

Associate Professor

Electrical Department, DTU

ACKNOWLEDGEMENT

With due respect, I express my deep sense of gratitude to my guide and motivator **Dr. Alka Singh**, Associate Professor, Electrical Department, Delhi Technological University for her co-operation and guidance. I acknowledge her invaluable help, suggestions in implementing the project. I am thankful to her for sparing her valuable time and encouraging me at every stage.

I would like to express my thankfulness to **Prof. Madhusudan Singh**, Head of Department for providing the laboratory and other facilities to carry out the project work. I am also thankful to all the faculty members of Electrical Engineering Department who enlightened me during my studies.

I am also thankful to **Mr. Manoj Badoni** (PhD. Research Scholar), **Ms. Nitu Dhyani**, **Mr. Ankit Yadav**, **Mr. Nimish Kumar** and **Mr. Sandeep Prajapati** for their valuable support and time. I am grateful to my parents for their moral support all time. They have been always supportive. I am also thankful to my friends for their unconditional support and motivation during this work.

Delhi, 2014 SACHIN KUMAR KESHARVANI

ABSTRACT

In the present scenario, non-linear loads are increasing day by day, due to which harmonics are being injected in the power system. This affects a number of sensitive loads connected to the system and affects their performance. In this work the simulations as well as hardware implementation has been done of a Distribution STATic COMpensator (DSTATCOM) for compensation of unbalanced loads and harmonic currents produced by non-linear loads. A proportional-integral (PI) controller is used for maintaining the DC-link voltage of the capacitor used in voltage source converter (VSC). The switching of VSC is done using Hysteresis Current Controller (HCC) based on indirect current control scheme. For generation of reference currents Fryze's current minimization algorithm, Adaptive filtering based on least mean square algorithms and Wiener filters have been studied and implemented. The simulations are carried out in Simulink/MATLAB and the hardware implementation of DSTATCOM is implemented with the help of dSPACE DS1104 R&D controller having TMS320F240 as a slave DSP. Both MATLAB-based and hardware implementation results are presented for demonstrating the steady state as well as dynamic load conditions.

CONTENTS

LIST OF FIGURES

LIST OF TABLES

ACRONYMS

DC	Direct Current
AC	Alternating Current
VSC	Voltage Source Converter
VSI	Voltage Source Inverter
PWM	Pulse Width Modulation
HCC	Hysteresis Current Control
IGBT	Insulated Gate Bipolar Transistor
KVA	Kilo Volt Ampere
THD	Total Harmonic Distortion
PCC	Point of Common Coupling
PI	Proportional Plus Integral
PLL	Phase Locked Loop
RMS	Root Mean Square
DVR	Dynamic Voltage Restorer
UPQC	Unified Power Quality Conditioner
DSTATCOM	Distribution Static Compensator
KW	Kilo Watt
MW	Mega Watt
GW	Giga Watt
PU	Per Unit
MS	Millisecond
MIN	Minute
LMS	Least Mean Square
ADALINE	Adaptive Linear Neural Network
MSE	Mean Square Error
FIR	Finite Impulse Response
APF	Active Power Filter
SVC	Static Var Compensator
LPF	Low Pass Filter

CHAPTER 1

INTRODUCTION

1.1 GENERAL

In present scenario the whole world faces energy shortages. There is a deficit between energy demand and energy supplied. The per capita energy consumption indicates the living standard of the society of the country and also it shows the development of the country. Every country is trying to harness the energy obtained from natural resources and maximize it. Due to the limited resources of the fossil fuels (coal, natural gas, oil, nuclear fuel etc.) the world is exploring renewable energy sources such as solar, wind, tidal, hydro, geothermal, biomass etc. However, problems such as high per unit cost act as major deterrents to the complete switchover to renewable energy.

Power engineers and researchers are now a days concentrating in the area of power electronics and power quality so that energy deficit problem can be overcome and good quality of power supply can be provided to the consumers at the least cost. Many devices such as FACTS (Flexible AC Transmission System) Devices and Custom Power Devices are in use at transmission and distribution level respectively. Literature review in this field, points to a number of solutions for mitigation of power quality issues.

This chapter highlights the power scenario in the world and India in particular. Facts and figures related to the different energy sources, installed capacity and contribution from renewable energy sources are provided for 2013-14. The next section lists the power quality problems in details and custom power devices.

1.1.1 Power Scenario in the World

The total installed capacity in the whole world is nearly equal to 5,144 GW (Giga Watt) as per 2013. China, U.S., Japan, Russia and India are the Top five countries in the list of installed generating capacity as it is shown in the Table 1.1. India holds the fifth position in the world. 55.75% of the total electricity of the world is produced by these five countries [1].

Table 1.1: Ranking list of countries on the basis of installed generating capacity in year-2013.

Country	Global Ranking	Installed Capacity (in GW)
China	1	1146
United States	2	1025
Japan	3	284.5
Russia	4	223.1
India	5	189.3
Germany	6	153.2
Canada	7	131.5
Italy	8	122.3
France	9	119.1
Brazil	10	106.2
Spain	11	102.5
United Kingdom	12	88.02
Korea	13	80.59
Mexico	14	59.33
Australia	15	56.94

1.1.2 Power Scenario in India

In India, the total installed capacity is 248.51 GW till the end of May 2014. Out of this total installed capacity, the non-renewable sources account for 87.55% and renewable sources constitute the remaining 12.45% of total installed capacity [2-4]. The state wise distribution of the total installed capacity (MW) is given in Table 1.2.

Table 1.2: Ranking list of 20 Indian states on the basis of installed generating capacity as of 31-Dec-2013.

Ranking	**State/Union Territory**	**Total Installed Capacity (MW)**
1	Maharashtra	32,505.98
2	Gujarat	26,269.12
3	Tamil Nadu	20,716.52
4	Andhra Pradesh	17,285.48
5	Uttar Pradesh	14,274.57
6	Rajasthan	14,059.12
7	Karnataka	13,940.66
8	Madhya Pradesh	12,902.35
9	West Bengal	8,708.82
10	Haryana	8,251.81
11	Punjab	7,614.95
12	Delhi Territory	7,500.79
13	Odisha	7,381.79
14	Chhattisgarh	6,864.91
15	Kerala	3,875.20
16	Himachal Pradesh	3,824.96
17	Uttarakhand	2,588.01
18	Jharkhand	2,579.86
19	Jammu and Kashmir	2,524.96
20	Bihar	2,198.13

Table 1.3 and Figure 1.1 give the breakup of total installed capacity of India as on 31 December 2013. Thermal sources contribute 68%, hydro has a share of 17% and the renewable source amounts to 13%. The remaining 2% of share is met by nuclear power sources.

:

Table 1.3: List of installed capacity from all the different energy sources as of 31 December 2013.

Energy Resource		**Installed Capaci1ty (MW)**
Thermal (Total)		159,793.99
	Coal	138,213.39
	Gas	20,380.85
	Diesel	1,199.75
Hydro		39,893.40
Nuclear		4,780.00
Renewable		29,462.55
Total		**233,929.94**

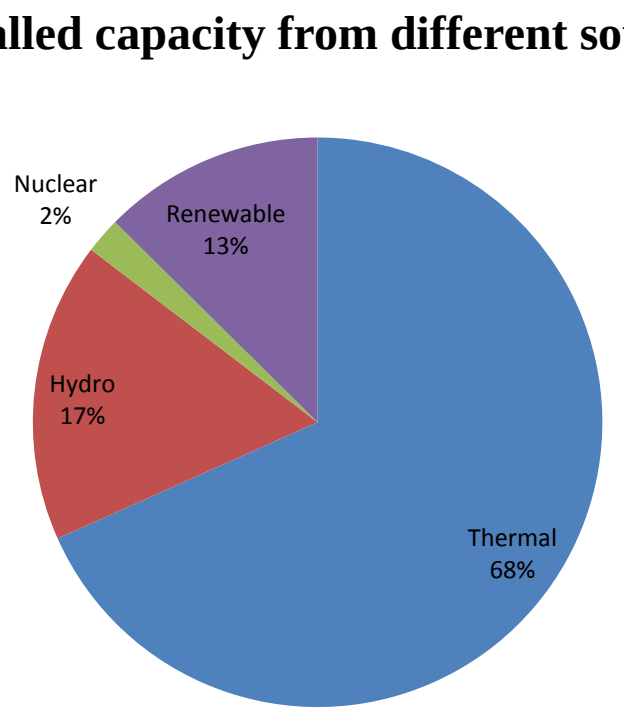

Figure 1.1: Breakup of electricity distribution in point of different resources in India.

Table 1.4: Total Renewable Energy Installed Capacity in India as of December 2013.

Renewable Energy Resource	**Installed Capacity (MW)**
Wind Power	20,149.50
Solar Power (SPV)	2,180.00
Small Hydro Power	3,763.15
Biomass Power	1,284.60
Bagasse Cogeneration	2,512.88
Waste to Power	99.08
Total	**29,989.21**

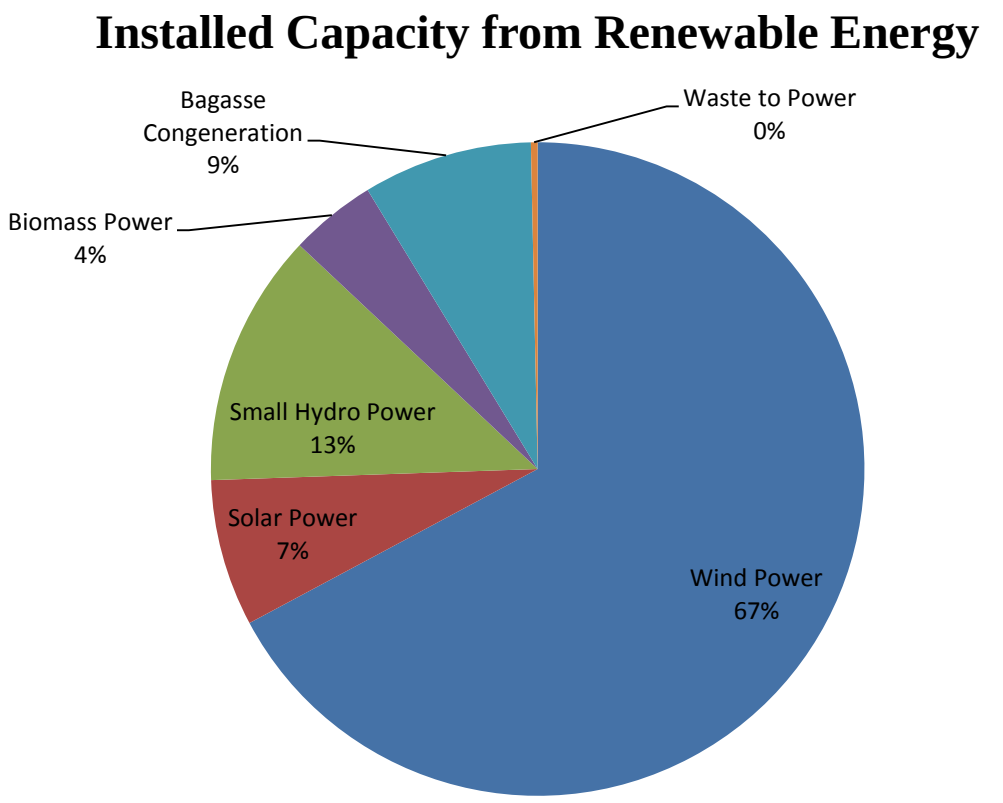

Figure 1.2: Breakup of installed capacity from renewable energy resources in India.

Table 1.4 and Figure 1.2 give a detailed distribution of renewable energy resources such as wind, solar power, small hydro, biomass etc. and their contribution in MW as well as percentage. The total installed capacity of renewable energy is 29,462 MW as per 31 December 2013 figures.

1.2 POWER SYSTEM LAYOUT AT DISTRIBUTION LEVEL

Figure 1.3 shows a typical power system network, in which generator/alternator, transmission lines, sub-transmission lines, transformers, loads are shown [5-7]. Different sections of the power system operate at different voltage levels due to transformer action. However, the entire power system operation and control takes place at a constant frequency of 50 Hz. T1 represents a step-up transformer and T2 &T3 represent step-down transformers. The entire power system is protected from faults & large transient conditions with the help of circuit breakers, relays and other protection devices.

At the distribution level, power generation generally takes place at 6 kV – 31 kV AC rms (phase to phase). It is then boosted up for transmitting the power through power transformer (T1) to a high voltage level typically 220kV, 400kV, 760kV etc. Then it is stepped down through power transformer (T2) at sub-transmission level i.e. 32kV to 132kV for the large factories and industrial customers. These industrial consumers have their own internal power distribution system to step down the voltage to 11kV, 3.3kV and 440V levels. The voltage is again stepped down through power transformer (T3) for transmitting power to the commercial and domestic consumers. The domestic and commercial consumers finally receive 440V (3-phase) or 230V (1-phase) power. The next section discusses power quality problems and some of the indexes for measurement of these.

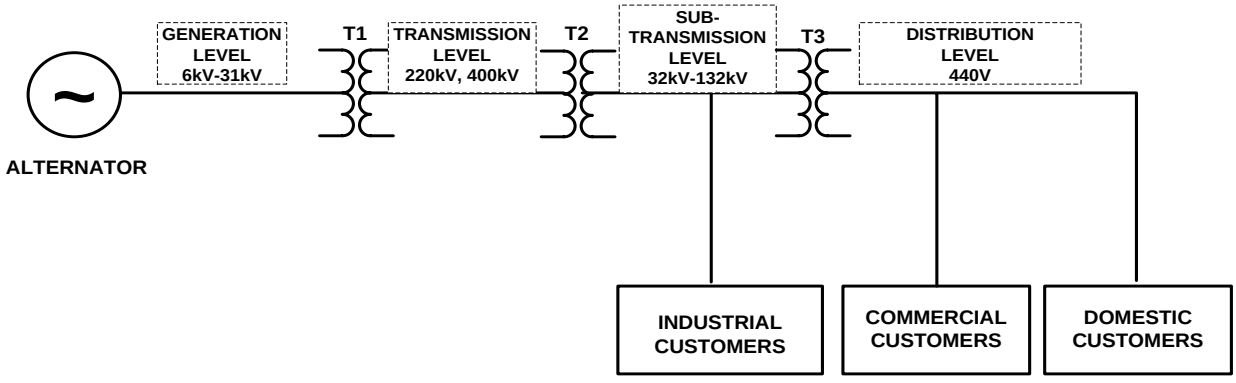

Figure 1.3: Layout of a typical power system layout.

1.3 POWER QUALITY PROBLEMS

Nowadays, the utility as well as the consumers are concerned about good power quality. Good reliable power supply is the backbone of industrial development of the country. As for Power supply voltage should have a fundamental sinusoidal waveform at frequency of 50 Hz and a constant rated voltage. Power qualities problems occur mainly due to harmonic injection and reactive power imbalance. However there are many other problems such as non-linear loading, lightning, large transients in loads, faults, electromagnetic interference (EMI), unbalanced loading in three phases, switching of capacitor banks etc. which distort the voltage & current waveforms further [5][8-10]. These are responsible for polluting the generating unit, transmission and distribution system. These unwanted events result in malfunctioning and damaging the sensitive devices. Many types of Active Power Filters (APF) are developed to solve the problems of current harmonics, reactive power compensation, power factor correction, voltage regulation etc. Many disturbances take place in power system and contribute to power quality problems. These are described below.

1.3.1 Transients

Transient [9] is the transition part of signal when it is changed from one steady state to another steady state. Transients can be divided into two categories, impulsive & oscillatory transients. Both transients occur in steady state condition of current, voltage or both. It is also called as surge.

1.3.1.1 Impulsive Transient

It is a sudden and non–power frequency change and it is unidirectional in polarity (in positive pulse or negative pulse).

1.3.1.2 Oscillatory Transients

It is a sudden and non–power frequency change that includes both positive and negative polarity values.

1.3.2 Short Duration Voltage Variations

This category of disturbances can be mainly subdivided into sag, swell and interruptions. [9]

1.3.2.1 Voltage Sag (Dip)

It is a reduction in rms voltage level to less than 0.9 pu at power frequency for few cycles ranging from 10 ms to 1 min.

1.3.2.2 Voltage Swell

It is defined as the increase in rms voltage level from 1.1 to 1.8 pu at the power frequency for few cycles ranging from 10 ms to 1 min.

1.3.2.3 Interruption

It is defined as the decrease in supply rms voltage to a level less than 0.1 pu for a duration not more than 1min.

These disturbances i.e. voltage sags, voltage swells and interruptions may further be classified [8] into three groups based on their duration.

- Instantaneous: 0.5–30 cycles
- Momentary: 30 cycles – 3 s
- Temporary: 3 s–1min

1.3.3 Long Duration Voltage Variations

Under this category of disturbances, three problems are listed.

1.3.3.1 Undervoltage

It is a reduction in rms voltage level to a value less than 0.9 pu at power frequency for duration more than 1 min. This effect is also referred to as Brownout.

1.3.3.2 Overvoltage

It is defined as the increase in rms voltage level from 1.1 to 1.8 pu at the power frequency for duration more than 1 min.

1.3.3.3 Interruption

When the supply rms voltage goes down to a level less than 0.1 pu for a duration of more than 1min, interruption is said to take place.

1.3.4 Voltage Imbalance

It is a condition, when the rms voltages of the three phases do not have equal magnitude.

1.3.5 Waveform Distortion

When the current or voltage waveforms are deviated from the perfect sinusoidal waveform, then waveform (signal) distortion is taking place. This is calculated and analyzed using total harmonic distortion (THD).

$$\text{THD} = \frac{\sqrt{\sum_{n=2}^{\infty} V_n^2}}{V_1} * 100\ \% \qquad (1.1)$$

where, V_1 is the fundamental rms voltage, V_n is the n^{th} harmonic rms voltage. The n^{th} harmonic has the frequency of 'n' times the fundamental frequency. According to IEEE 519-1992 standard, the voltage and current waveforms have an acceptable power quality if the THD is less than 5%.

Waveform distortion may be due to harmonics and inter-harmonics. Those sinusoidal current or voltage waveforms whose frequency is integral multiples of fundamental frequency i.e. 50 Hz are called Harmonics. The sinusoidal current or voltage waveforms, whose frequency is not an integral multiple of fundamental frequency, are called Inter-Harmonics. The presence of a dc voltage or current in an ac power system is termed DC-offset. Notching may also be present, which takes place at the time of commutation when the alternating current is switched from one phase to another phase in a 3-phase ac to dc converter. This results in a momentary short circuit and distortion of voltage and current signals.

1.3.6 Voltage Fluctuations

Loads that show rapid, continuous variations in load current result in voltage variations referred to as flicker.

1.3.7 Power Frequency Variations

It shows the deviation of the frequency of the power system from the fundamental frequency. It depends on the balance between the real power generation and consumption. The accepted tolerance in power frequency is ±1% of the fundamental frequency.

1.4 CUSTOM POWER DEVICES

The application of power electronics based controllers at the power distribution level for the benefit of a customer or group of customers is called Custom Power Devices. Family of custom power devices [5, 11] can be categorized broadly into:-

- Shunt device or Distribution Static compensator (DSTATCOM)
- Series device or Dynamic voltage restorer (DVR)
- Hybrid device or Unified power quality conditioner (UPQC)

These compensating devices are mainly used for active filtering of harmonics, load balancing, power factor correction and voltage regulation. The connection of these custom power devices (DSTATCOM, DVR and UPQC) at the distribution power system is illustrated in Figure 1.4.

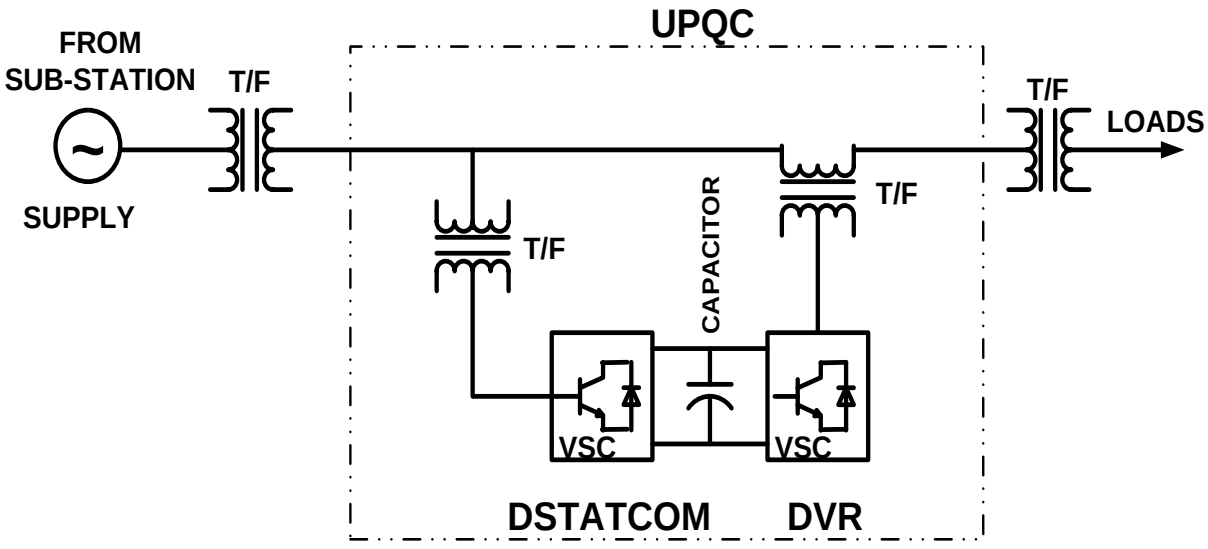

Figure 1.4: Configuration of Custom Power devices in distribution system.

1.4.1 DISTRIBUTION STATIC COMPENSATOR

A DSTATCOM has the ability to perform multiple functions such as load balancing, harmonics elimination and regulating the voltage of the point of common coupling (PCC) by transferring the reactive power from the PCC to DSTATCOM or DSTATCOM to PCC. DSTATCOM is a solid state DC/AC power switching converter that consists mainly of a 3-phase voltage source converter (VSC) having six insulated gate bipolar transistors (IGBT) with associated anti-parallel diodes. DSTATCOM has structure and function similar to STATCOM in the transmission system. It is connected in shunt with the power system at the PCC. It rapidly injects a current of desired frequency, phase and magnitude into the grid.

Figure 1.5 shows the typical structure of DSTATCOM. It consist a voltage source converter, energy storage device and interfacing inductors etc. Many control algorithms, can be used to adjust voltage and phase and achieve a good control on reactive power exchange and active power transfer between the ac system and DSTATCOM.

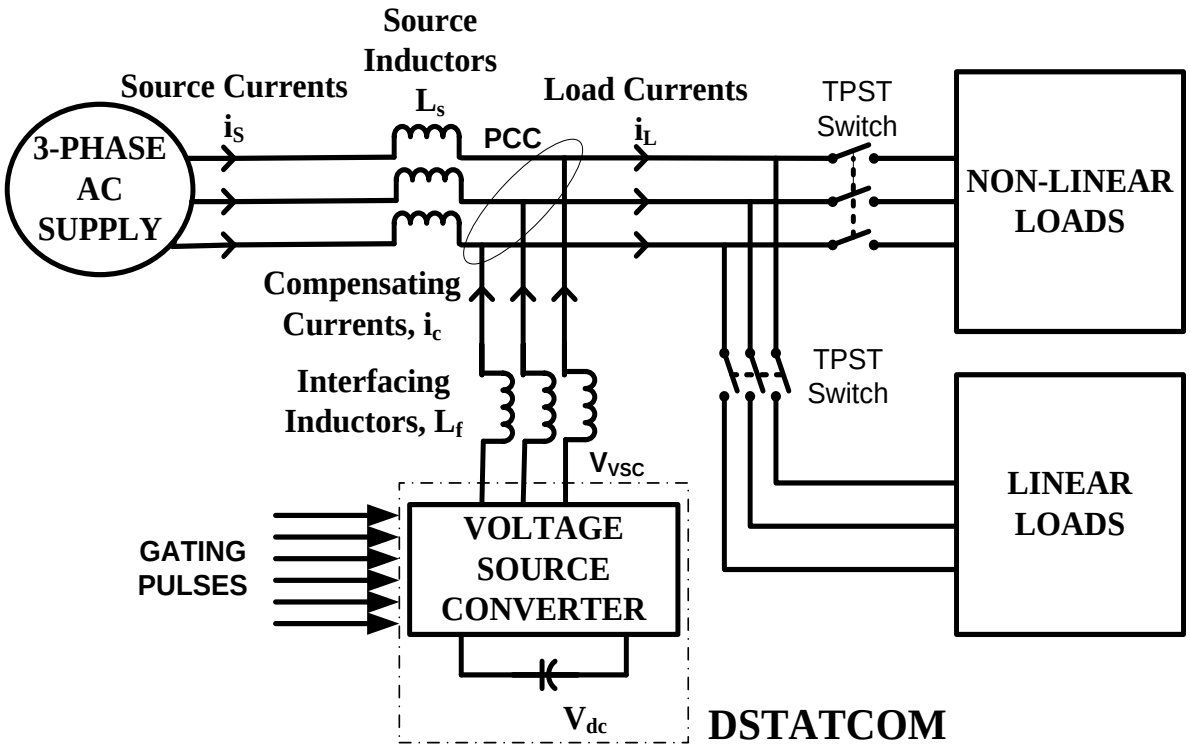

Figure 1.5: Schematic diagram of DSTATCOM.

Various functions of DSTATCOM include:

1. Compensation of reactive power and voltage regulation
2. Power factor correction
3. Current harmonics Compensation

Figure 1.5 shows the schematic diagram of DSTATCOM, in which i_c is the compensator current, i_S is the source current and i_L is the load current. The impedance between the PCC and the output terminal of the VSC is $Z_L=(R_L+jX_L)$. Where, X_L (= $2\pi fL_f$) is the inductive impedance of the line between these two terminals and f is the instantaneous operating frequency of the system. L_f is inductance value of the interfacing inductors.

The shunt injected current i_c can be written as shown in equation (1.2).

$$i_c = i_L - i_S = \frac{V_{VSC} - V_{PCC}}{Z_L} \quad (1.2)$$

where, V_{VSC} is the ac voltage of the output terminals of VSC and V_{PCC} is the voltage at the PCC.

1.4.1.1 OPERATION MODES OF DSTATCOM

DSTATCOM can work in four modes [12, 13] as explained below by vector diagrams.

(i) Capacitive mode or reactive power release

(ii) Inductive mode or reactive power absorption

(iii) Active power release

(iv) Active power absorption

$$P \text{ (Active Power)} = (V_{PCC}V_{VSC}/X_L)\sin\delta \quad (1.3)$$

$$Q \text{ (Reactive Power)} = (V^2_{PCC}/X_L) - (V_{PCC}V_{VSC}/X_L)\cos\delta \quad (1.4)$$

where, δ is the angle difference between the PCC voltage (V_{PCC}) and the ac output voltage of the converter (V_{VSC}). Depending upon the voltage difference and the power angle, these modes of operations are decided. Power angle decides the active power release & active power

absorption and the voltage difference between the two terminals decides the capacitive mode & inductive mode.

If the power angle of the PCC is greater than the power angle of the output voltage of the DSTATCOM, then the active power will flow from the PCC to DSTATCOM and vice-versa. In case of reactive power transfer; if the PCC voltage is greater than the DSTATCOM voltage then the reactive power will flow from the PCC to DSTATCOM and the DSTATCOM will be working as in inductive mode and vice versa. For a capacitor based VSC, V_{PCC} & V_{VSC} have the same phase, but for compensating the active power consumption (inverter switching and the loss of transformer) a little difference has been kept, so that that much real power can be transferred from the power system. Expressions (1.3) and (1.4) express the active and reactive power flow between the two terminals PCC and VSC.

1.4.1.2 DESCRIPTION OF DSTATCOM OPERATION

DSTATCOM is connected to the distribution system via interfacing inductors, L_f. A DC-link capacitor provides constant DC link voltage [14]. In the system, the DC link voltage of VSC is kept fixed at 200V and for regulating the dc link voltage a dedicated dc voltage Proportional-Integral (PI) controller is used.

Some power losses occur in the voltage source converter. So for compensating these losses, active power should flow from source of the network. The block diagram of DC voltage regulator is shown in Figure 1.6, in which a PI-controller is used for maintaining the voltage of DC capacitor. V_{dcref} is the desired DC link voltage and it is set as 200V.

Transfer function of the PI-controller is;

$$T_s = K_p + K_i/s \quad (1.5)$$

where, K_p is called proportional gain and K_i is called integral gain of the controller.

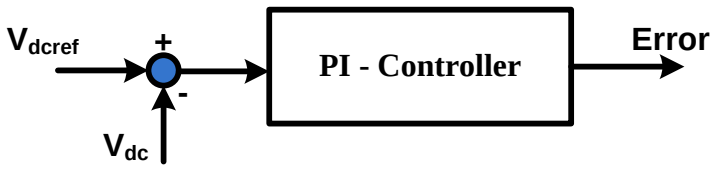

Figure 1.6: Block diagram of DC voltage regulator.

The DC to AC converter produces the output voltage at the terminal of DSTATCOM with the energy storage capacitor. The DC voltage at the converter produces a set of controllable three phase output voltages at the power frequency. The reactive power exchange between the PCC and DSTATCOM is controlled by changing the magnitude of the voltage produced. DSTATCOM is a shunt compensator which can be controlled so that it can inject suitable compensation currents. As compared to conventional static var compensator (SVC), it responses faster and produces reactive power at low voltage.

The energy ($E_{dc)}$ required by the DC link capacitor to charge from actual voltage (V_{dc}) to the reference value (V_{refdc}) can be computed from equation (1.6) below

$$E_{dc} = 0.5*C_{dc}(V^2_{dcref} - V^2_{dc}) \quad (1.6)$$

where, C_{dc} is the capacitance of dc link capacitor.

DC Power (P_{dc}) required from the capacitor is calculated as

$$P_{dc} = K_p (V^2_{dcref} - V^2_{dc}) + K_i\int(V^2_{dcref} - V^2_{dc})dt \quad (1.7)$$

1.4.1.3 DESIGN OF DSTATCOM

The performance of VSC is depends upon the parameters of the components associated with the VSC [15-17]. Here some of the related parameters are discussed, such as DC bus voltage V_{dc}, DC storage capacitance C_{dc} and interfacing inductance L_f.

1.4.1.3.1 Reference DC Link Voltage

Capacitor is used as the energy storage device and its voltage is decided according to the working voltage level of the ac distribution system. DC voltage level is selected for achieving good tracking performance. The DC link voltage is maintained at $1.3V_m$, where V_m (i.e. 110V) is maximum value of line to line voltage of the 3-phase system. The reference DC link voltage is taken as 200V for the study.

$$V_{dcref} = 1.3V_m \quad (1.8)$$

1.4.1.3.2 Storage Capacitance

At the time of transients the dc capacitor supplies or demands energy from the ac system to maintain the quality of source power. For calculating the capacitance value, suppose controller works after the n cycles, so nST is the maximum possible energy capacity of the

capacitor. This much energy can be supplied to or absorbed from the system. Where S is the maximum load rating and T is system time period. Hence,

$$\frac{1}{2}C_{dc}(V_{dcref}^2 - V_{dcm}^2) = nST \quad (1.9)$$

$$C_{dc} = \frac{2nST}{(V_{dcref}^2 - V_{dcm}^2)} \quad (1.10)$$

where, V_{dcm} is the maximum allowable voltage.

1.4.1.3.3 Interfacing Inductance

Neglecting the resistance of the interfacing inductors, inductors are designed to provide good performance at maximum switching frequency, at which the HCC is operated. So considering these aspects interfacing inductance L_f [15] is given by,

$$L_f = \frac{V_{dcref}}{4hf_{max}} \quad (1.11)$$

where, 2h is ripple in the current and f_{max} is maximum switching frequency achieved by HCC.

1.4.1.4 GENERATION OF PULSES FOR SWITCHING THE GATES

The generation of switching pulses is done using the HCC [18]. The conventional hysteresis band (HB) current control technique has proven to be most suitable for controlling DSTATCOM. The HB current controller decides the switching logic pattern of the DSTATCOM, according to:

If, $i_S < (i_S^* - HB)$ upper switch is OFF, lower switch is ON.

If, $i_S > (i_S^* + HB)$ upper switch is ON, lower switch is OFF.

where, i_S is the measured current; i_S^* is the reference current.

1.4.2 DYNAMIC VOLTAGE RESTORER

It is a device which is connected in the series with the load [19]. It is used for compensation of supply voltage by regulating if there are problems on the supply side of the distribution system. Desired voltage of required amplitude, phase and frequency is injected by DVR between grid and load. It is a very powerful device, which has the ability to mitigate the voltage swells and sags at the PCC. The difference between DVR and DSTATCOM how they are connected (i.e. series or shunt). DVR employs a transformer in series with the ac system,

but DSTATCOM is connected as shunt compensator with the ac system as shown in Figure 1.7. Some functions of DVR are:

(i) Reactive Power Compensation
(ii) Voltage Regulation
(iii) Compensation for Voltage sags and Swells
(iv) Unbalance Voltage Compensation (for 3-phase systems)

The VSC based DVR produces three phase voltages such that the voltage across the load terminals can be regulated at the desired reference value. The equation of injected voltage can be written as equation no. (1.12).

$$V_{DVR} = V_{LOAD} + Z_S I_S - V_S \quad (1.12)$$

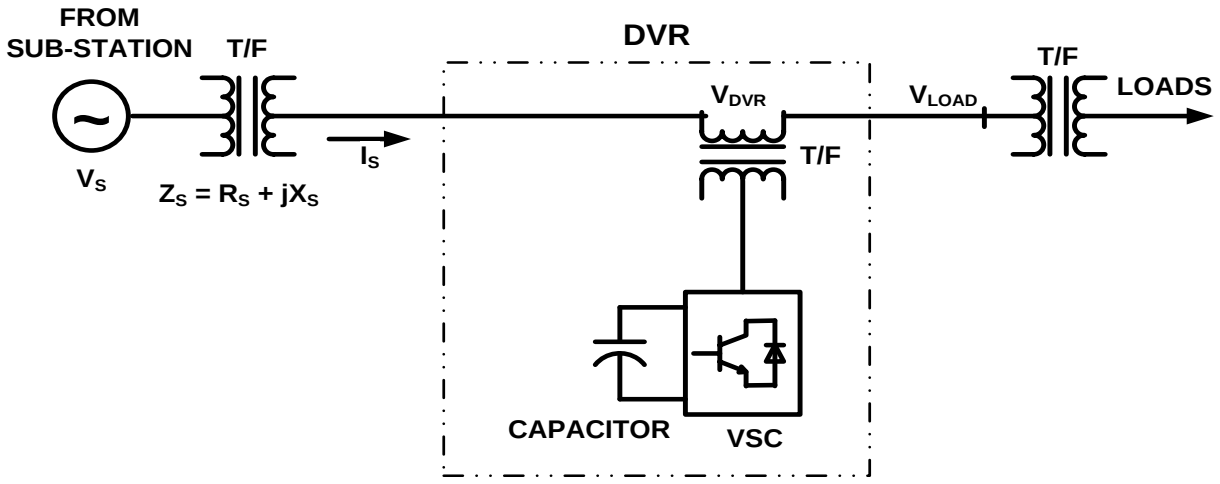

Figure 1.7: Schematic diagram of DVR.

1.4.3 UNIFIED POWER QUALITY CONDITIONER

UPQC is a hybrid compensator having the capability to inject shunt currents and series voltage to the system. It consists of both series and shunt converters connected to the same DC link [20, 21]. It is a very powerful device which can mitigate both disturbances of current and voltage which may affect many sensitive loads. The basic structure of the UPQC is shown in Figure 1.8.

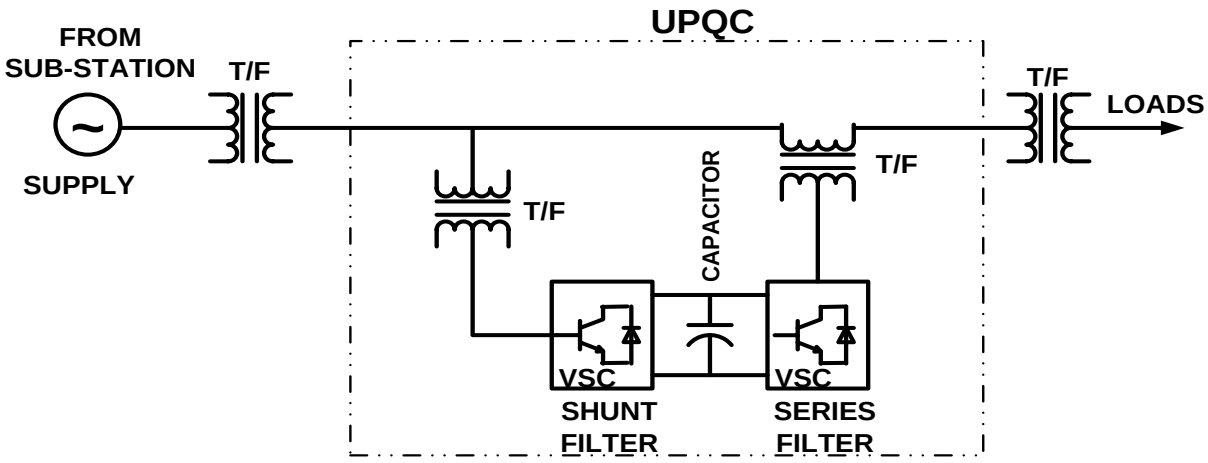

Figure 1.8: Schematic diagram of UPQC.

The functions of UPQC include

(i) Reactive Power Compensation

(ii) Voltage Regulation

(iii) Compensation for Voltage Sag and Swell

(iv) Unbalance Compensation for current and voltage (for 3-phase systems)

(v) Neutral Current Compensation (for 3-phase 4-wire systems)

1.5 CONCLUSION

In this chapter, the energy scenario of the world and India in particular has been discussed. A typical power distribution structure layout is explained at generation, transmission, sub-transmission and distribution level. Power quality problems are mentioned and some of them include transients, short duration and long duration voltage variations, voltage imbalance, waveform distortions, harmonics, inter-harmonics, fluctuations in voltage and frequency. Custom power devices i.e. DSTATCOM, DVR and UPQC are also discussed in this chapter. Operation modes, parameters and controlling of DSTATCOM are studied.

Power engineers are deeply concerned about power quality issues and the need of following standards. Several solutions have been suggested in literature for alleviating these problems, and some of these are discussed in the next chapter.

CHAPTER 2

LITERATURE SURVEY AND PROPOSED SYSTEM

2.1 GENERAL

In this section, many research papers, journal papers and books have been reviewed on many emerging areas of the power system. Mainly focused on the power quality problems and possible solutions, active and passive filters, custom power devices (DSTATCOM, DVR and UPQC), PI-controller, some conventional algorithms and some adaptive filter algorithms for the generating the reference currents.

2.2 LITERATURE SURVEY

Arindam Ghosh and **Gerard Ledwich** [5] have characterized of electric power quality, analyzed about conventional mitigation methods. Custom power devices (DSTATCOM, DVR and UPQC) have been described in detail with their structure and control schemes.

Ravilla Madhusudan and **G. Ramamohan Rao** [10] have presented Modeling and Simulation of a DSTATCOM for mitigating the problems of Power Quality like voltage sag and swell based on sinusoidal PWM.

Pudi Sekhar, K. Venkateswara Rao and **T.Devaraju** [11] have presented models of custom power devices, namely DVR, DSTATCOM and PWM switched autotransformer, applied them to mitigate voltage dip which is very prominent as per utilities are concerned.

Parmar Hiren.S, Vamsi Krishna.K and **Ranjit Roy** [12] presented the modeling and control of the STATCOM and its dynamics response to system oscillations cause by a three-phase fault. It has been shown that the STATCOM can be very effective in damping power system oscillations.

Pinaki Mitra, Ganesh Kumar and **Venayagamoorthy** [13] have presented a novel adaptive control strategy based on based on artificial immune system (AIS) for the DSTATCOM for maintaining the voltage at the point of common coupling.

Mahesh K. Mishra and **K. Karthikeyan** [14] have proposed a fast-acting DC link voltage controller, which is based on the energy of a dc-link capacitor. The state-space modeling of the DSTATCOM is discussed for carrying out the simulation studies.

Chandan Kumar and **Mahesh K. Mishra** [15] have discussed about ratings of the VSC and the interfacing inductors used between VSI and PCC in a 3-phase 4-wire system.

Srinivas Bhaskar Karanki, Nagesh Geddada, Mahesh K. Mishra and **B. Kalyan Kumarhave** [16] proposed a hybrid topology of DSTATCOM, which is very much capable for compensating the load at a lower DC link voltage at condition of non-stiff source. Detailed explanation is given to design the filter parameters. In this research paper, the validation of the presented method is done through simulation and experimental studies in a three phase distribution system.

Mahesh K. Mishra and **K. Karthikeyan** [17] have presented a controller which acts very fast to control the DC-Link Voltage and maintain the voltage to the reference value in a three-Phase four-wire system consisting DSTATCOM. In this paper, DSTATCOM is compensating ac unbalanced and non-linear load for preventing the harmonics to enter to the source.

George Adam, Alina Georgiana Stan and **Gheorghe Livinţ** [18] have presented a new adaptive hysteresis band controller for three phase shunt active power filters implemented using the Fuzzy logic. The simulations were carried in MATLAB under two load configurations, balanced and unbalanced.

Mr.Y.Prakash and **Dr. S.Sankar** [19] proposed emergency and efficient control in distribution system, which is analyzed by using a multifunctional DVR with control strategy.

V. Khadkikar, A. Chandra, A. O. Barry and **T. D. Nguyen** [20] have presented a brief study about the UPQC during power quality problems like voltage sag and voltage swell in the distribution system. One of the specialties of UPQC is that it can inject voltage to the PCC voltage from 0º to 360º. Depending on the phase angle of the injected voltage, UPQC can be able to absorb or inject the active power.

Bharath Babu Ambati and **Vinod Khadkikar** [21] introduced an optimum method to design a unified power-quality conditioner (UPQC) system with the minimum possible VA rating based on the compensation requirements. A set of generalized VA loading equations for the UPQC is derived, which are valid for all of the UPQC control approaches (such as UPQC-P, UPQC-Q, and UPQC-VA_{min}).

Hirofumi Akagi, Edson Hirokazu Watanabe and **Mauricio Aredes** [22] have described in detail about the Instantaneous Power Theory, Shunt, Series and Hybrid Filters. The structures and controls of many filters have been explored.

Karuppanan P, and **Kamala Kanta Mahapatra** [23] have presented shunt active filter for improving the power quality such as harmonics compensation and reactive power compensation because of non-linear loads. A novel compensation control scheme, generalized Fryze currents minimization based on positive sequence voltage detector is implemented and it is able to compensate harmonics and reactive power.

C.N. Rowe, T.J. Summers, R.E. Betz and **D. Cornforth** [24] presented on control scheme to control power flow in a standalone micro-grid, which is Power frequency droop method. This paper compares the effect of instantaneous and Fryze power calculations on the operation of a three phase, two inverter micro-grid.

Mauricio Aredes and **Luis F. C. Monteiro** [25] described a novel control strategy i.e. the sinusoidal Fryze current control strategy based on minimization method equations, together with a robust synchronizing circuit (PLL circuit) for shunt active filters.

Alexandru Bitoleanu and **Mihaela Popescu** [26] presented paper on the Reference Current Methods Calculation and their Implementation for the shunt filters. Many control schemes have been described such as the Fryze's theory, the theory of Fryze-Buchholz-Depenbrock, the so-called generalized theory of instantaneous reactive and non-active powers, the Currents' Physical Components Theory (CPC) and the Conservative Power Theory (CPT).

Bhim Singh, Sunil Kumar Dube, Sabha Raj Arya, Ambrish Chandra and **Kamal Al-Haddad** [27] have presented a comparative study of the performance of two weight updating ADALINE (Adaptive Linear Neural Network) based on adaptive algorithm LMS and Fuzzy logic based variable step size LMS used for harmonic current detection using VSC based DSTATCOM.

Maryclaire Peterson, Brij N. Singh and **Parviz Rastgoufard** [28] presented many topologies of active and passive filter to provide suggestion to power engineers and researches. Mathematical models of active and passive filter topologies are presented in this paper and developed simulation models with the C programming language.

Alexander D. Poularikas and **Zayed M. Ramadan** [29] have dealt with many methods of adaptive filtering like, Wiener filters, Newton and steepest-descent method, the LMS algorithms, least square and recursive least-squares signal processing.

Simon Haykin [30] has talked about many methods in the field of adaptive filter theory. In this book many filters and methods have been described. Some of those are Wiener

filters, method of steepest descent, LMS and normalized adaptive filters, method of least squares, recursive least-squares adaptive filters etc.

Bhim Singh and **Jitendra Solanki** [31] have implemented the hardware of a shunt active filter (SAF) for compensating harmonic currents, reactive power and unbalanced loading produces by the loads. SAF is controlled using current estimator based on an adaptive-linear-element (Adaline) for maintaining source currents sinusoidal and unity power factor. Three-phase load currents are sensed and using least mean square (LMS) algorithm-based Adaline, online calculation of weights is performed and these weights are multiplied by the unit vector templates, which give the fundamental-frequency real component of load currents, which are used in to produce the reference currents.

Djaffar Ould Abdeslam, Patrice Wira, Jean Mercklé, Damien Flieller and **Yves-André** [32] have proposed an efficient and reliable neural APF for estimation and compensation of harmonic distortions. The filter is proposed based on Adaline neural networks which are associated with different independent blocks. They have introduced a neural method based on Adalines for the online extraction of the voltage components to recover a balanced and equilibrated voltage system and three different methods for harmonic filtering. These three methods efficiently separate the fundamental harmonic from the distortion harmonics of the measured currents.

Sireesha N., K. Chithra and **Tata Sudhakar** [33] implemented an adaptive filter based on LMS algorithm. In this paper convergence and stability, choice of step size and other parameter related to filter are discussed.

Bhim Singh, Sabha Raj Arya, Ambrish Chandra and **Kamal Al-Haddad** [34] have implemented an adaptive filter in a three-phase DSTATCOM used for compensation of linear/nonlinear loads in a three phase distorted voltage AC mains. The proposed filter which is based on adaptive synchronous extraction is used for extraction of fundamental active and reactive power components of load currents in estimating the reference supply currents. This control algorithm is implemented on a developed DSTATCOM for reactive power compensation, harmonics elimination, load balancing and voltage regulation under linear and nonlinear loads.

P. Wira, D. Ould Abdeyslam and **J. Mercklé** [35] have compared different variants of the least mean squares (LMS) algorithm. The objective consists in finding the best compromise between on-line learning and computational costs. Indeed, an algorithm with low

computational complexity for updating Adalines weights is required for a real-time implementation of a modular neural Active Power Filter. This filtering scheme is inserted in an electric distribution system to identify and compensate for harmonic distortions. The overall complexity of the neural frameworks is evaluated in terms of basic operators such as adders, multipliers and signum functions.

Farzad Nekouei, Neda Zargar Talebi, Yousef S. Kavian and **Ali Mahani** [40] implemented hardware of adaptive least mean square (LMS) filter considering fixed step size and self-correcting adaptive filter. The comparative analysis is given in terms of convergence speed, hardware utilization and maximum frequency.

Leonardo S. Resende, João Marcos T. Romano and **Maurice G. Bellanger** [41] proposed a new structure for split transversal filtering and introduced the optimum split Wiener filter. A power normalized, time-varying step-size least mean square (LMS) algorithm, which exploits the nature of the transformed input correlation matrix, is proposed for updating the adaptive filter coefficients. Simulation results enable us to evaluate the performance of the multi-split LMS algorithm.

2.3 PROPOSED SYSTEM CONFIGURATION

A three phase system of 110V line-to-line, 50 Hz frequency is taken as power circuit of the studied system. At the point of common coupling, a three phase, 3 legs DSTATCOM is connected. The DSTATCOM is implemented using a universal bridge consisting of IGBTs with anti-parallel diodes. Interfacing inductors of 3.2mH are used connecting the voltage source converter to power circuit. Validation of control scheme has been done by simulation as well as experimentally. LEM (LV-25) voltage sensors are used for sensing PCC voltages and LEM (LA-25) current sensors are used for sensing source and load currents. LV-25/SP5 voltage sensor having capacity of 1500V is used for sensing DC link voltage. The control scheme is implemented in dSPACE DS1104 R&D controller having TMS320F240 as a slave DSP. A three phase bridge rectifier having series RL branch on DC side with different R values and 100mH fixed inductor is used as non-linear load. The current rating of load can vary from 1A to 10A. The simplest controller in the form of a PI-controller is used to regulate the voltage of dc link to its reference value of 200V.

Figure 2.1 shows the block diagram of DSTATCOM connected to the system. The DSTATCOM works on the principle of shunt compensation and injects the current based on

the objective to be achieved. If the controller is to be designed for harmonic compensation, then it is controlled to inject current distortions in the load current equal in magnitude but opposite in sign. Thus, it cancels the harmonic distortions coming from the load to the source at the PCC, which results in improved power quality of the source. The following equation shows the instantaneous source current (i_S) and the source voltages (v_S) are

$$i_S(t) = i_L(t) - i_c(t) \quad (2.1)$$

$$v_S(t) = V_m \sin\omega t \quad (2.2)$$

where, i_S, i_L, i_c, v_S and V_m are the instantaneous source current, load current, compensator current, source voltage and peak value of the source voltage. The load current signal waveform can be analyzed by Fourier series method of decomposition. It can be analyzed as sum of two terms, the first one corresponding to fundamental component and second term corresponds to harmonics component.

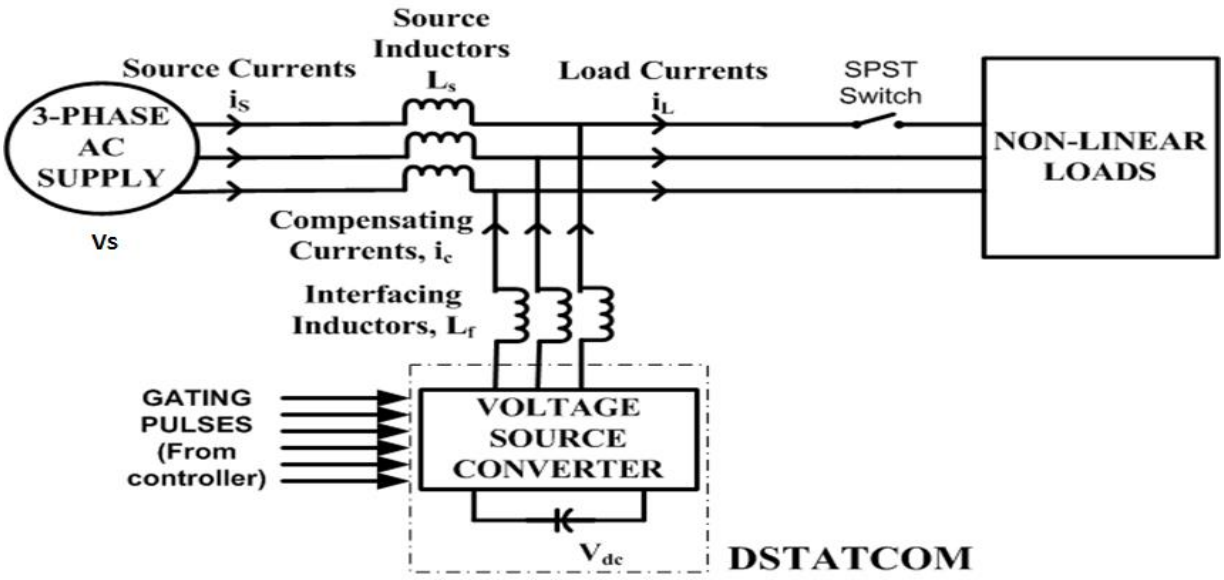

Figure 2.1: DSTATCOM implemented in distribution system with the non-linear loads.

$$i_L(t) = \sum_{n=1}^{\infty}(I_n \sin(n\omega t + \phi n))$$

$$= I_1 \sin(\omega t + \phi_1) + \sum_{n=2}^{\infty}(I_n \sin(n\omega t + \phi_n)) \quad (2.3)$$

= Fundamental component + Harmonic components

The second component of the load current (equation 2.3) is produced by the compensator in phase opposition to improve the power quality of the supply current.

The unit templates are computed using system voltages. The amplitudes of the PCC voltages (V_t) is estimates as follows:

$$V_t = \sqrt{\frac{2}{3}}(v^2_{ta} + v^2_{tb} + v^2_{tc}) \quad (2.4)$$

The unit vector in-phase of PCC voltages (v_{Sa}, v_{Sb}, v_{Sc}) are computed as follows:

$$u_{pa} = v_{ta}/v_t \; ; \; u_{pb} = v_{tb}/v_t \; ; \; u_{pc} = v_{tc}/v_t \quad (2.5)$$

The unit vectors in quadrature with the PCC voltages are derived using the unit vectors in-phase PCC voltage as follows:

$$u_{qa} = - u_{pb}/\sqrt{3} + u_{pc}/\sqrt{3} \quad (2.6)$$

$$u_{qb} = \sqrt{3}\, u_{pa}/2 + (u_{pb} - u_{pc})/2\sqrt{3} \quad (2.7)$$

$$u_{qc} = - \sqrt{3}\, u_{pa}/2 + (u_{pb} - u_{pc})/2\sqrt{3} \quad (2.8)$$

2.4 CONCLUSION

Literature survey related to the work has been done in many fields related to power system, which include mainly power quality problems, possible solutions, custom power devices (DSTATCOM, DVR and UPQC), many controllers based on different algorithms. Some algorithms like Fryze current minimization algorithm, Adaptive filtering based on LMS and Wiener filtering scheme have been studied.

CHAPTER 3

CONDUCTANCE BASED FRYZE ALGORITHM

3.1 FRYZE CURRENT MINIMIZATION ALGORITHM [22-28]

The VSC may be connected in two ways. The series connection of VSC provides voltage compensation and the shunt connection provides current compensation of the load. This conductance based Fryze current minimization controller based shunt compensator is presented here. This controller is better than the Instantaneous reactive power theory (IRPT) based controller which was introduced by H. Akagi. IRPT controller is computational complicated due to involvements of steps like park transformation, dq-transform and dq-inverse transform. Some power losses occur in the voltage source converter. So for compensating these losses, active power should flow from source of the network. Figure 3.1 shows the block diagram of Generalized Fryze Current Minimization Algorithm, in which a DC voltage regulator using PI-controller is used for maintaining the voltage of DC capacitor. The output of the PI-controller i.e. G_{loss} is then used for the calculation of the active currents. G_{loss} component represents the loss component. V_{dcref} is the desired DC link voltage and it is set as 200V.

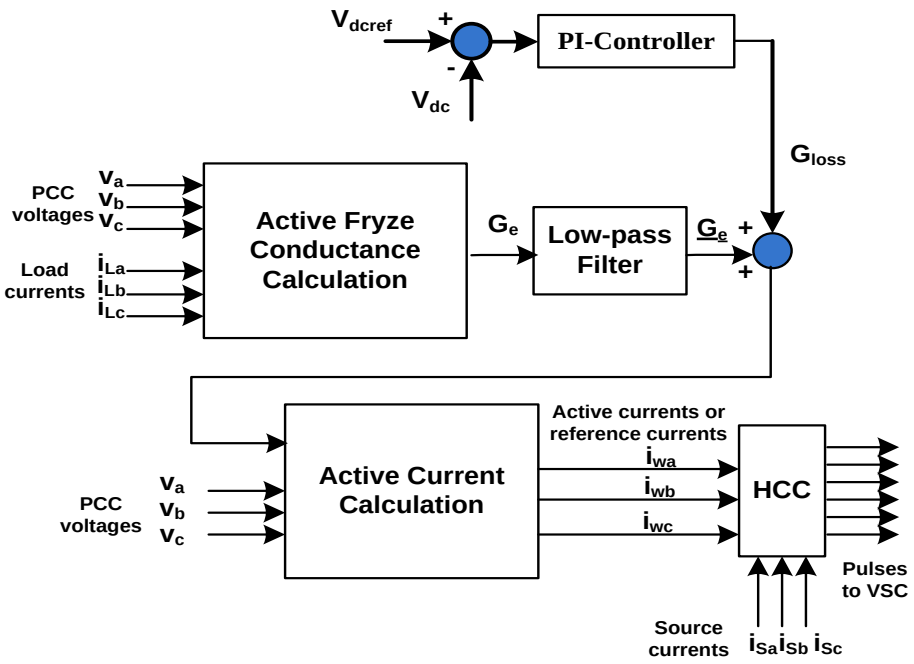

Figure 3.1: Block diagram of Generalized Fryze Current Minimization Algorithm.

In the Fryze current minimization control scheme, active Fryze Conductance calculation is done with the PCC voltages (v_a, v_b, v_c) and the load currents (i_{La}, i_{Lb}, i_{Lc}) according to the given formula (3.1).

$$G_e = \frac{v_a.i_{La} + v_b.i_{Lb} + v_c.i_{Lc}}{v_a^2 + v_b^2 + v_c^2} \quad (3.1)$$

where, G_e is the average value of conductance, v_a, v_b and v_c are the sensed phase voltages of the PCC and i_{La}, i_{Lb} and i_{Lc} are the sensed load currents. The calculated value of average conductance value is passed through a low-pass filter (LPF) of frequency 50Hz for filtering the fundamental part of the conductance. So the output of the filter i.e. G_e is added with the G_{loss} to get the net conductance G.

$$G = G_e + G_{loss} \quad (3.2)$$

The obtained value of G is multiplied with the phase voltages v_a, v_b and v_c to get the active currents (reference currents) i.e. i_{wa}, i_{wb} and i_{wc}.

$$i_{wa} = (G_e + G_{loss}).\ v_a \quad (3.3)$$

$$i_{wb} = (G_e + G_{loss}).\ v_b \quad (3.4)$$

$$i_{wc} = (G_e + G_{loss}).\ v_c \quad (3.5)$$

These active currents are passed through the hysteresis current controller (HCC) for generating six gating pulses to operate the six IGBTs of the three legs VSC. The complete control scheme is represented in the Figure 3.1. The next chapters discuss the simulation results and hardware implementation based on Fryze's algorithm.

3.2 SIMULATION RESULTS

Figure 3.2 shows the simulation model made on Simulink /MATLAB. In which a three phase power system, non-linear load and DSTATCOM are connected. Figure 3.3 shows the implementation of the Fryze current minimization algorithm in Simulink MATLAB with DC voltage regulator and HCC. Figure 3.4 shows the Simulink model in MATLAB, which compares sensed source current and reference currents for producing the gating pulses of the VSC.

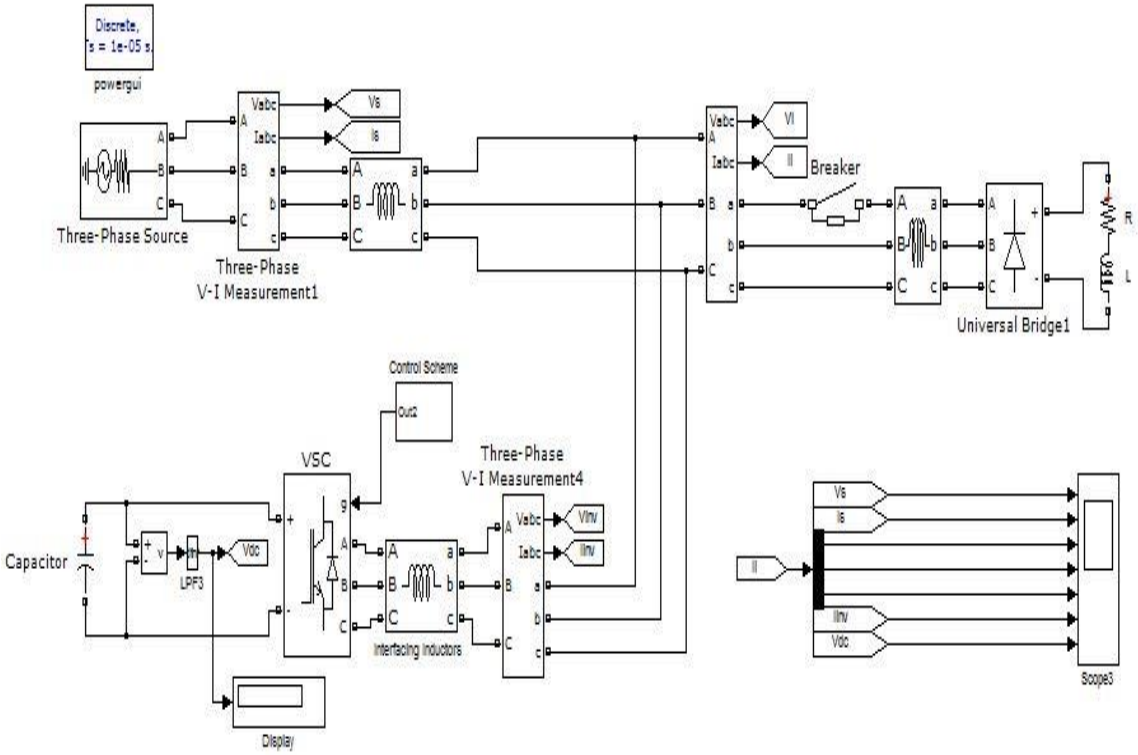

Figure 3.2: Simulation model of the distribution system.

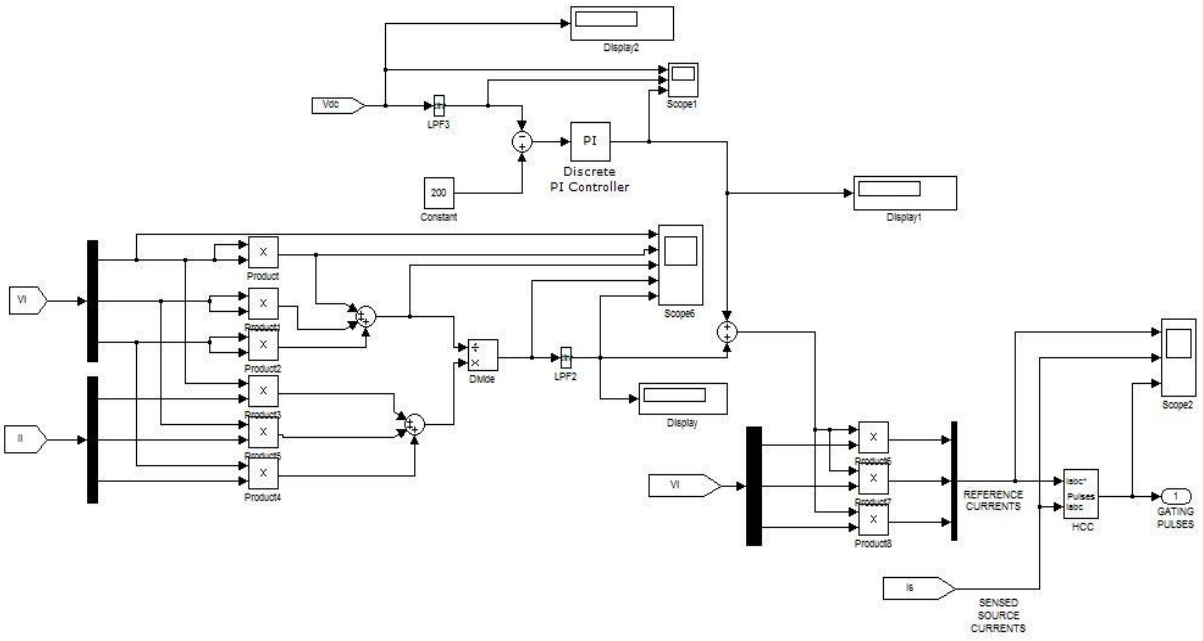

Figure 3.3: Simulation model of the Fryze current minimization algorithm.

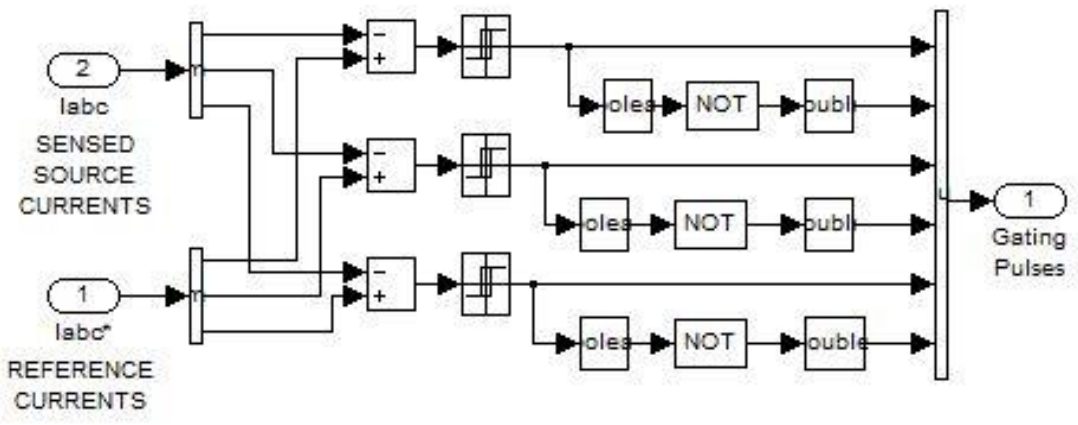

Figure 3.4: Simulink model of Hysteresis Current Controller.

Figure 3.5 shows the simulation results for the developed system at steady state and unbalanced conditions. In which various plots of supply voltages (V_s), supply currents (i_S), phase 'a', 'b' & 'c' load currents (i_{La}, i_{Lb} & i_{Lc}), compensator currents (i_c) and dc link voltage (V_{dc}). The system is controlled by Fryze current minimization scheme. Till 0.4 the load is balanced and the load currents have THD of 27.93% with the implementation of DSTATCOM the dc link is maintain to 200V and the supply currents are observed to balanced and sinusoidal. The THD of supply current is 2.54% in steady state condition.

Figure 3.6 and Figure 3.7 show the FFT analysis for THD of load current and supply current of phase 'a'. At t=0.4 sec phase 'a' load is removed for a duration of 0.1 sec. The subplot of phase 'a' current shows a magnitude of zero during this duration. Under the sudden load change the dc link voltage of the VSC overshoots to approximately 205V but settles down quickly to its reference value of 200V.

During the dynamic load change condition, the supply currents are still observed to be sinusoidal, balanced and reduced in magnitude as compared to the steady state condition. The compensator injects higher currents to account for the unbalance in load current. At t=0.5 sec once again the phase 'a' of load is restored and hence the supply current is increase in magnitude as before.

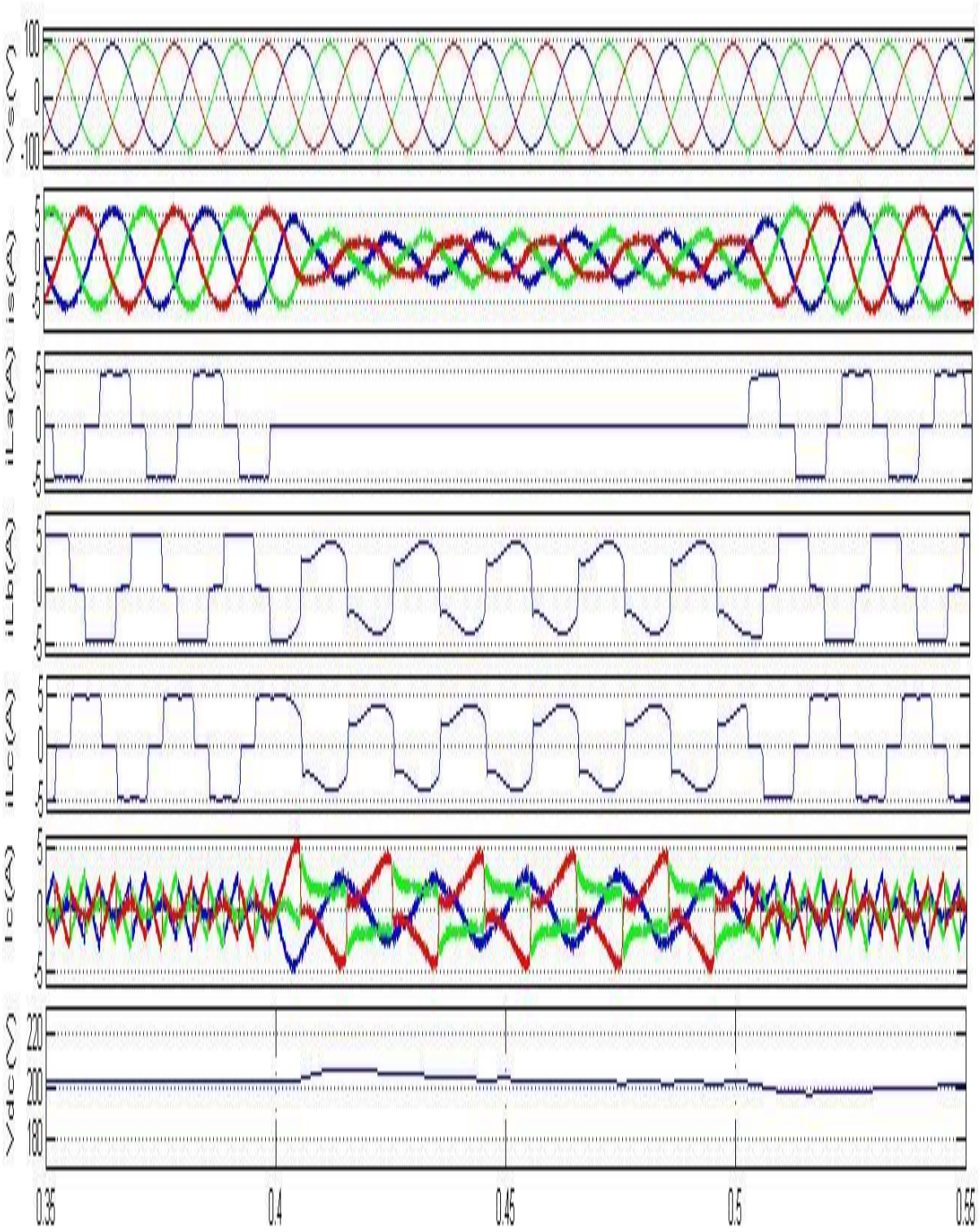

Figure 3.5: Dynamic response of the system with non-linear load condition.

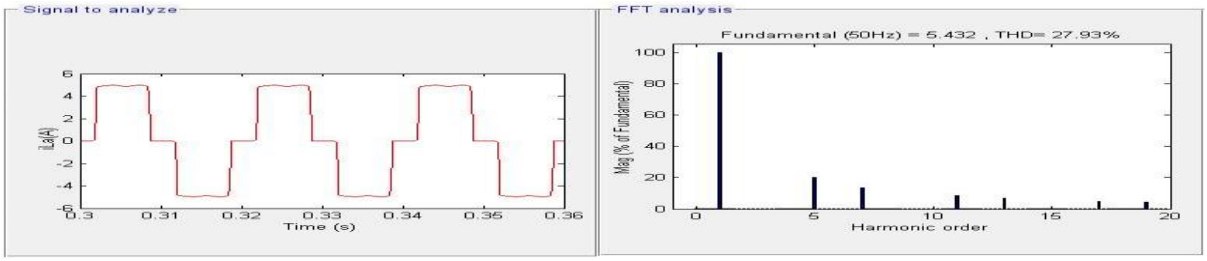

Figure 3.6: FTT analysis is shown for the THD of phase ‘a’ load current.

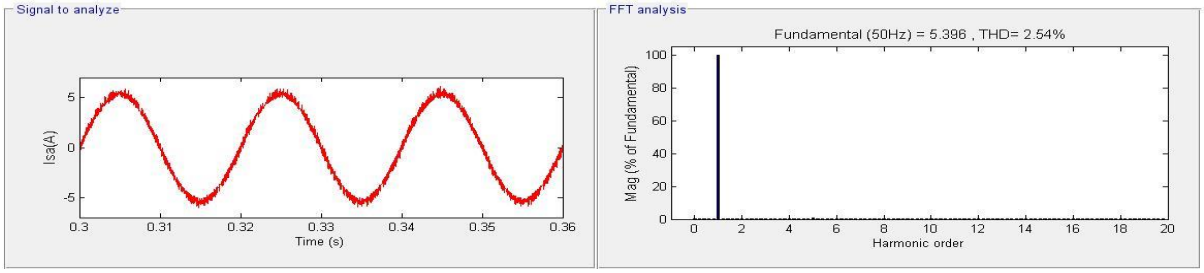

Figure 3.7: FTT analysis is shown for the THD of phase ‘a’ source current.

3.3 HARDWARE RESULTS

Results are taken with non-linear load in balanced and unbalanced conditions, which are shown on Tektronix TDS2014B CRO. Figure 3.8 to Figure 3.16 show the results of hardware implementation with the controller based on Fryze’s algorithm. Figure 3.8 shows the signal plots for the phase ‘a’ supply current, load current and the compensator current on the CRO in steady state condition. It can be clearly observed that the supply current is sinusoidal even with non-linear load. The compensator injects highly distorted current corresponding to the harmonic component of the load current and thus improves the power quality at the supply end.

Figure 3.9 and Figure 3.10 show the signal plots of source current (i_{Sa}), load current (i_{la}), compensator current (i_{ca}) of the phase ‘a’ and dc link voltage V_{dc} under dynamic load conditions of load removal and load addition respectively. Figure 3.9 shows the magnitude of the load current is reduced to zero during load removal. The compensator current increased during this interval to maintain a reduced but sinusoidal supply current. The dc link is also found to settle in less than one cycle. The results for load addition are shown in similar manner in Figure 3.10. On comparing the simulation results (shown in Figure 3.5) with the hardware results (shown in Figure 3.8 - Figure 3.10) a good match is obtained.

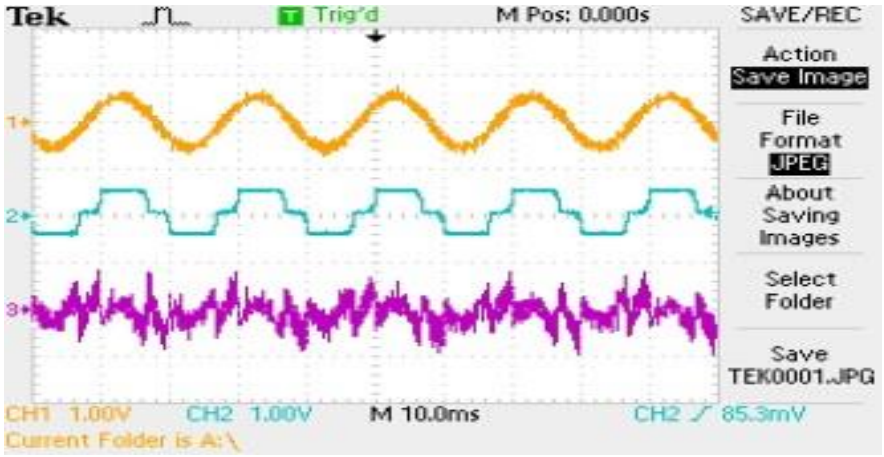

Figure 3.8: Signal plots of i_{Sa}, i_{La} and i_{ca} on the CRO.

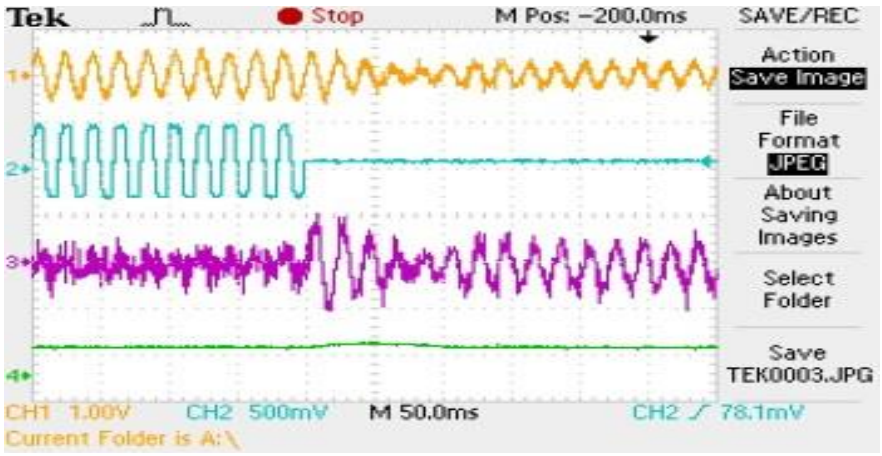

Figure 3.9: Signal plots of i_{Sa}, i_{La}, i_{ca} and V_{dc} on the CRO of load removal condition.

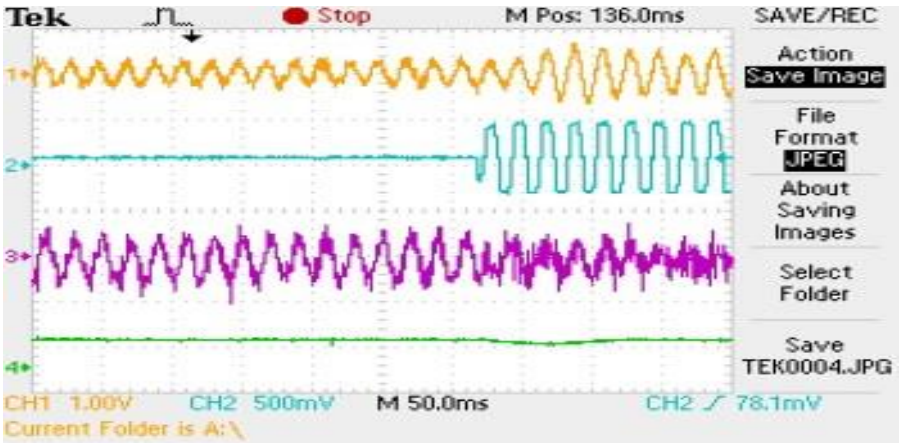

Figure 3.10: Signal plots of i_{Sa}, i_{La},i_{ca} and V_{dc} on the CRO of load addition condition.

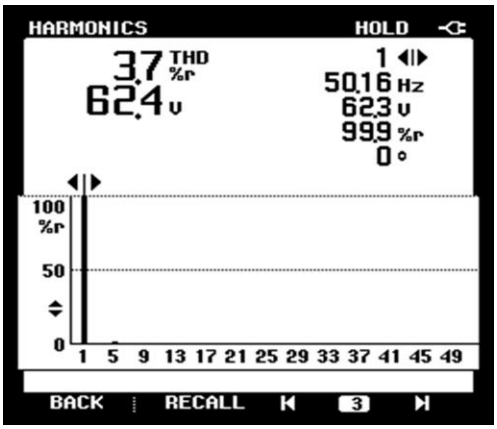

Figure 3.11: THD of the phase 'a' supply voltage.

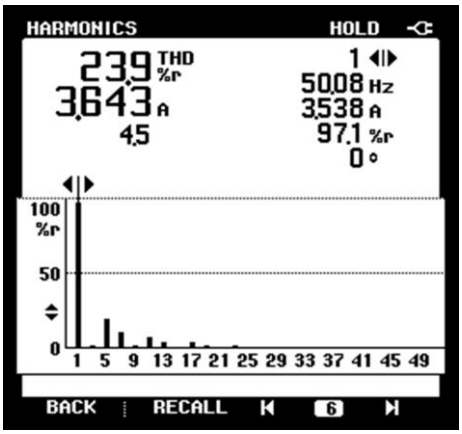

Figure 3.12: THD of the phase 'a' load current.

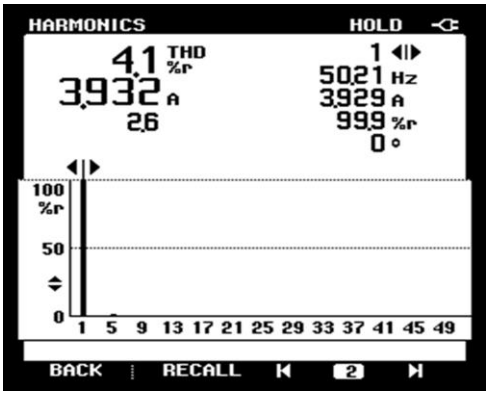

Figure 3.13: THD of phase 'a' supply current.

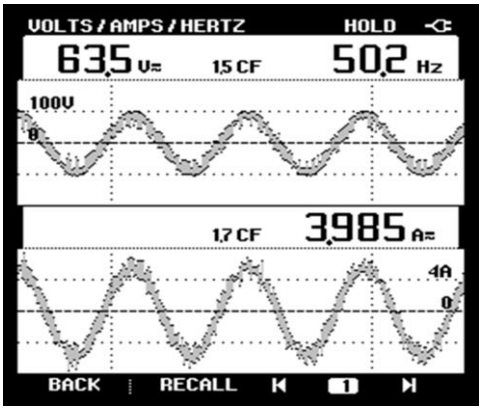

Figure 3.14: Waveforms of the v_{Sa} and i_{Sa}.

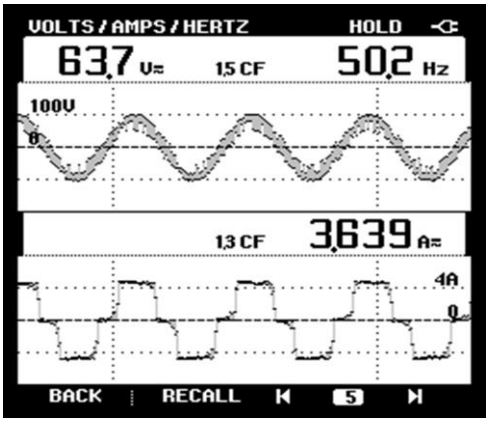

Figure 3.15: Waveforms of the v_{Sa} and i_{La}.

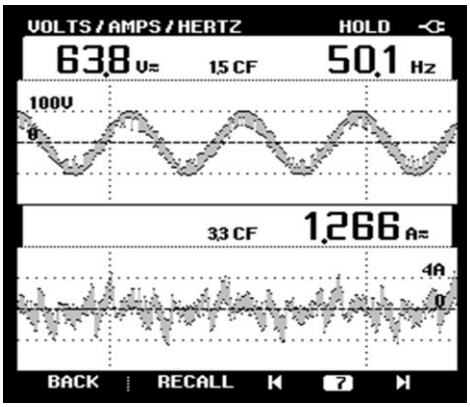

Figure 3.16: Waveforms of the v_{Sa} and i_{ca}.

Figure 3.11 to figure 3.13 show the waveforms and THD for various currents and voltages. Figure 3.11 shows the THD of source voltage of phase ‘a’, which is observed as 3.7%. Figure 3.12 shows the THD of load current of phase ‘a’, which is observed as 23.9%. Figure 3.13 shows the THD of source current of phase ‘a’, which is observed as 4.1%.

Figure 3.14 shows the waveform for supply voltage and supply current of phase ‘a’. It can be observed clearly that both of them are in phase. The compensator is able to achieve unity power factor also. Figure 3.15 shows the voltage and load current waveform of phase ‘a’. Since the non-linear load is connected in experimental set up the load current waveform is observed with harmonics. Figure 3.16 shows the waveforms for supply voltage and compensator current of phase ‘a’. The figure clearly shows the compensator injects highly distorted current to cancel the harmonics in load current.

3.4 CONCLUSION

Hardware implementation of prototype DSTATCOM is implemented and realized with generalized Fryze current minimization control strategy with non-linear loads and it is observed that power quality of the system is improved satisfactorily. Reference currents are extracted by sensing the load currents from current sensors by conductance formula. The switching signals for the gate of IGBTs are derived from HCC. The voltage of dc capacitor is maintained by the help of PI controller in all the cases. The conductance based Fryze control scheme is found to be very effective in reducing the THD within 5% of supply current as per the IEEE-519 standards. Moreover, the scheme works well under dynamics of load changes, load unbalancing and removal of load too. The simulation results based on Fryze’s Scheme match well with the hardware developed model of the system.

CHAPTER 4

ADAPTIVE LMS FILTER

4.1 GENERAL

In this chapter adaptive least mean square filtering is described in detail, particularly three schemes are studied i.e. simple LMS, Sign-regressor LMS and Normalized LMS. Simulation results of all three schemes are described and compared.

4.2 ADAPTIVE FILTERING BY THE LMS ALGORITHM

The least mean-square (LMS) algorithm was developed by Widrow and Hoff in 1960. This algorithm is a member of stochastic gradient algorithms, and because of its robustness and low computational complexity, it has been used in a wide spectrum of applications [29-41].

The LMS algorithm has the following most important properties:

1. Its form is simple and can also be implemented easily. It is capable of delivering high performance during the adaptation process.
2. Its iterative procedure involves:
   a. computing the output of an finite impulse response (FIR) filter produced by a set of tap inputs ($\mathbf{x}(k)$, filter coefficients),
   b. generation of an estimated error by comparing the output of the filter to a desired response, d(k) and
   c. adjusting the tap weights ($\mathbf{W}(k)$, filter coefficients) based on the estimation error.
3. It includes a step-size parameter (μ), that must be selected properly to control stability and convergence speed of the algorithm.
4. It is stable and robust for a variety of signal conditions.

For updating the tap weights, the following expressions of learning rules are used.

$$\mathbf{W}(k+1) = \mathbf{W}(k) + 2\mu\mathbf{x}(k)[d(k) - \mathbf{x}^{T}(k)\mathbf{W}(k)] \quad (4.1)$$

$$\mathbf{W}(k+1) = \mathbf{W}(k) + 2\mu\mathbf{x}(k)[d(k) - \mathbf{W}^{T}(k)\mathbf{x}(k)] \quad (4.2)$$

$$\mathbf{W}(k+1) = \mathbf{W}(k) + 2\mu e(k)\mathbf{x}(k) \quad (4.3)$$

where,

filter output: $$y(k) = \mathbf{W}^{T}(k)\mathbf{x}(k) \quad (4.4)$$

error: $e(k) = d(k) - y(k)$ (4.5)

filter taps at time k: $\mathbf{W}(k) = [W_0(k)\ W_1(k)\ W_2(k)\ \ldots\ldots\ W_{M-1}(k)]^T$ (4.6)

input data: $\mathbf{x}(k) = [x(k)\ x(k-1)\ x(k-2)\ \ldots\ldots\ x(k-M+1)]^T$ (4.7)

The algorithm defined by equations (4.3), (4.4) and (4.5) constitute the adaptive LMS algorithm. The algorithm at each iteration requires that **x**(k), d(k) and **W**(k) are known. The LMS algorithm is a stochastic gradient algorithm if the input signal is a stochastic process.

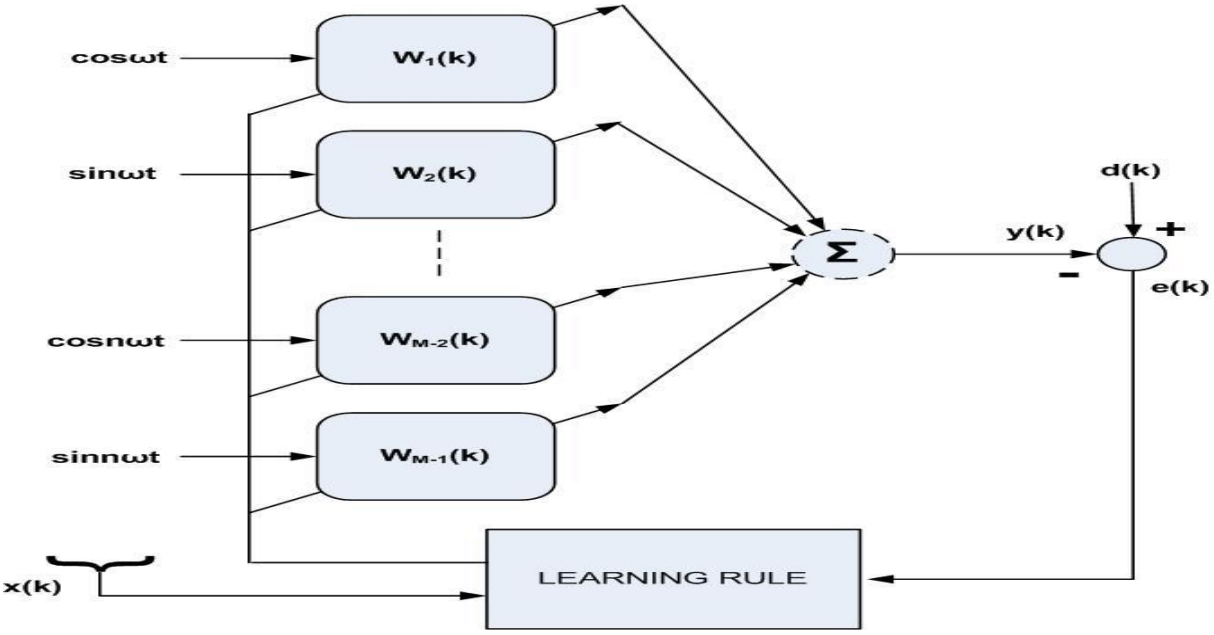

Figure 4.1: LMS realization.

Using the LMS approach, the harmonic current components are extracted from the actual load currents. Addition of these harmonic current components gives the estimated load current. The simple structure of adaline is a very powerful tool in the field of adaptive filtering. The adalines can be used for extracting the harmonic current components from the load currents of the system. Using this technique, for every harmonic, two adalines are used which corresponds to the active and reactive component of the harmonic. Weight training is carried out using LMS algorithm. This method is fast and effective because of parallel computations taking place simultaneously.

In this chapter two LMS algorithms have been studied, simulated and compared. The measured current of each phase is decomposed into the Fourier series as follows:

$$i_L = \sum_{n=1}^{\infty}(I_{n1}\cos n(\omega t - \alpha) + I_{n2}\sin n(\omega t - \alpha)) \quad (4.8)$$

From this expression, we can define the fundamental and harmonics components. n=1 represents the fundamental component. The fundamental current will be written as

$$i_{Lf}(t) = I_{11}\cos(\omega t - \alpha) + I_{12}\sin(\omega t - \alpha) \quad (4.9)$$

where, α is the phase angle between the current and the load voltage, $I_{11}$and I_{12} are the sine and cosine frequency components of fundamental current, $I_{n1}$and I_{n2} are the cosine and sine frequency components of n_{th} harmonic of the distortion current. Figure 4.2 shows the adaline diagram, in which W_{11}, W_{12}, W_{n1} and W_{n2} are the weights corresponding to amplitudes of fundamental active component, fundamental reactive component, n^{th} harmonic active component and n^{th} reactive component of the load current.

The harmonic current can be calculated as in equation (4.10),

$$i_{Lh}(t) = i_L(t) - i_{Lf}(t) \quad (4.10)$$

The extraction of the harmonic components is done by using an Adaline for each phase.

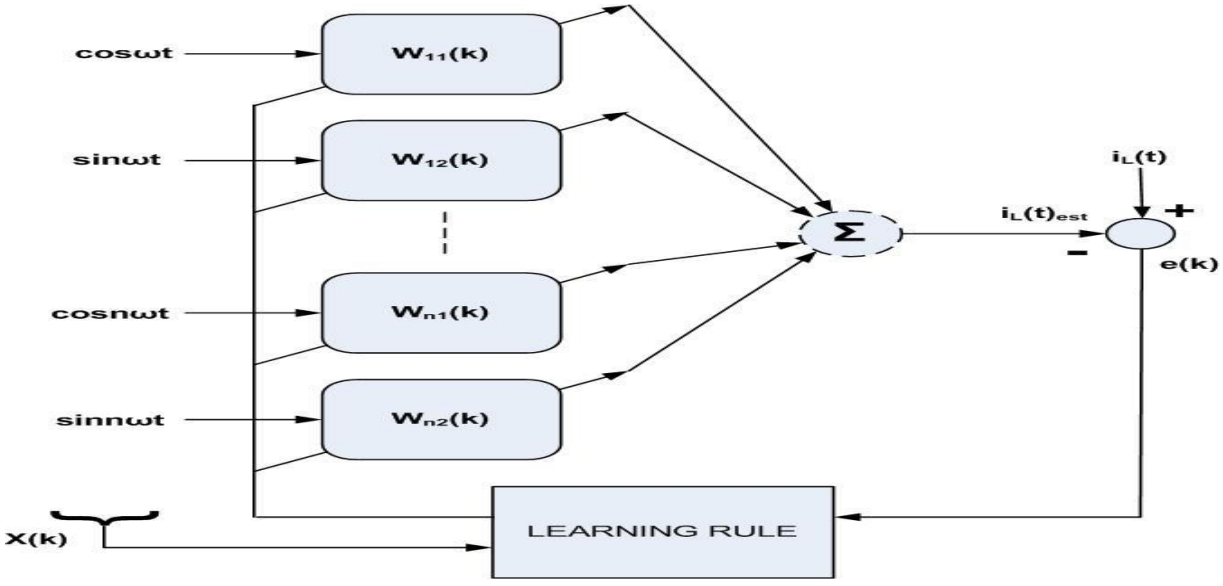

Fig. 4.2: Adaline for harmonic extraction using the direct method.

4.3 LMS ALGORITHM

For the decomposition of weights corresponding to the all components of currents, the adalines are adopted with the help of LMS learning rule written as follows.

$$\mathbf{W}(k+1) = \mathbf{W}(k) + 2\mu e(k)\mathbf{x}(k) \tag{4.11}$$

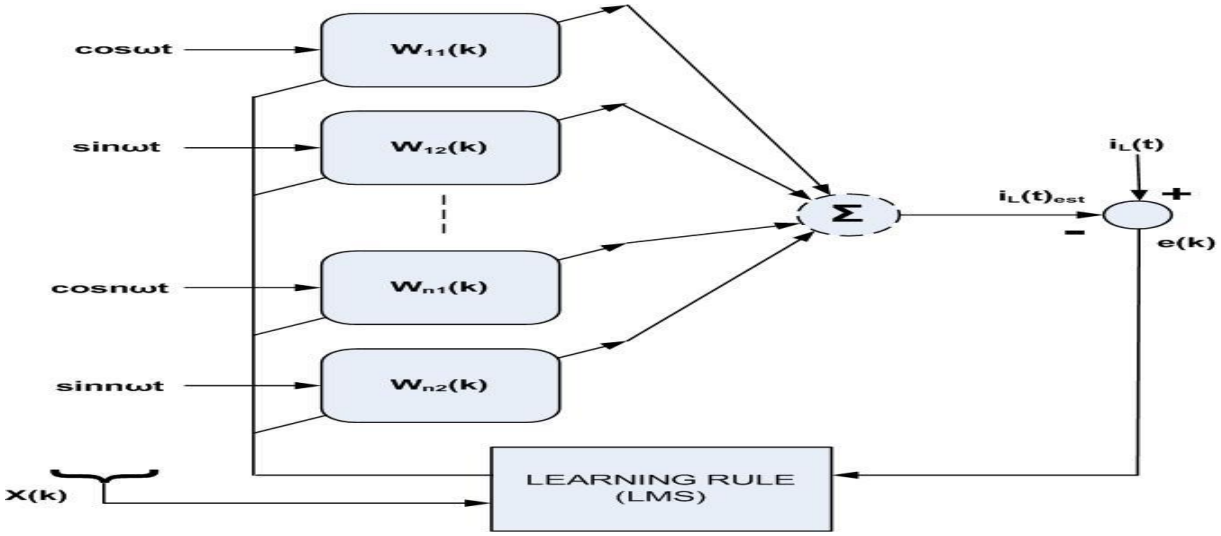

Figure 4.3: Realization of adaptive filter based on least mean square method.

Figure 4.3 shows the realization of adaptive filter based on LMS algorithm for minimizing the error between actual load current and estimated load current.

4.3.1 SIMULATION RESULTS

Results of the simulation are explained for three cases. First case corresponds to balance loading, second to unbalance loading and third to again balanced loading. The unbalancing (load removal) is done in phase 'c' in DSTATCOM to the load side at 0.2 sec for interval of 0.2 sec and at 0.4 sec the load is reconnected.

Figure 4.4 shows the simulation results for the developed system at steady state and unbalanced conditions. In which various plots of supply voltages (V_s), supply currents (i_S), phase 'a', 'b' & 'c' load currents (i_{La}, i_{Lb} & i_{Lc}), compensator currents (i_c) and dc link voltage

(V_{dc}). The system is controlled by simple LMS algorithm based adaptive filter. Till 0.2 the load is balanced and the load currents have THD of 26.23% with the implementation of DSTATCOM the dc link is maintain to 200V and the supply currents are observed to balanced and sinusoidal. The THD of supply current is 2.42% in steady state condition. The unbalancing (load removal) is done in phase 'c' in DSTATCOM to the load side at 0.2 sec for interval of 0.2 sec and at 0.4 sec the load is reconnected. It can be seen that the waveforms of source currents are sinusoidal during balance loading as well as unbalance loading..

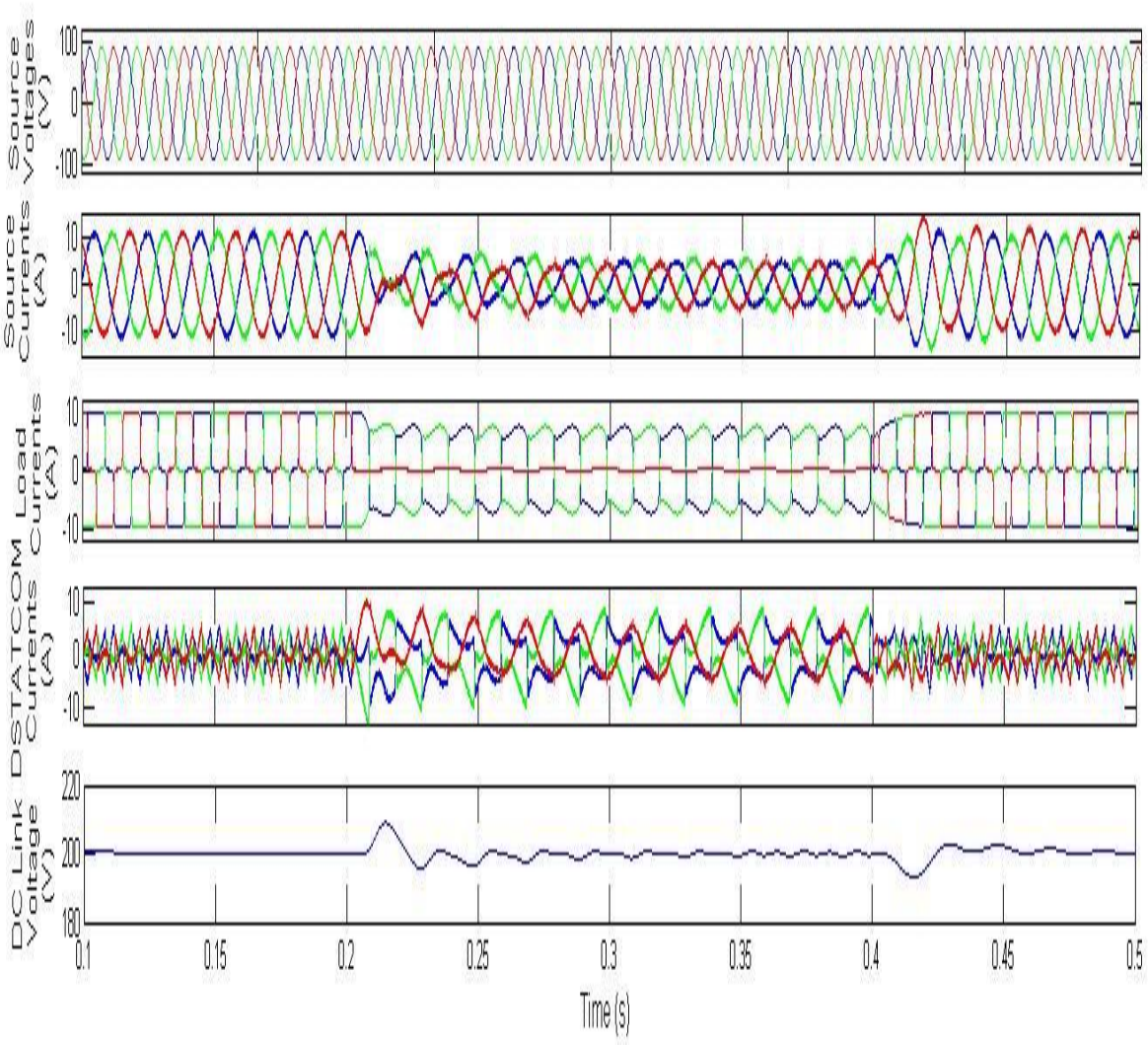

Figure 4.4: Dynamic response of the system is shown with non-linear load condition. Waveforms of source voltages, source currents, load currents, compensator currents and DC link voltage are shown.

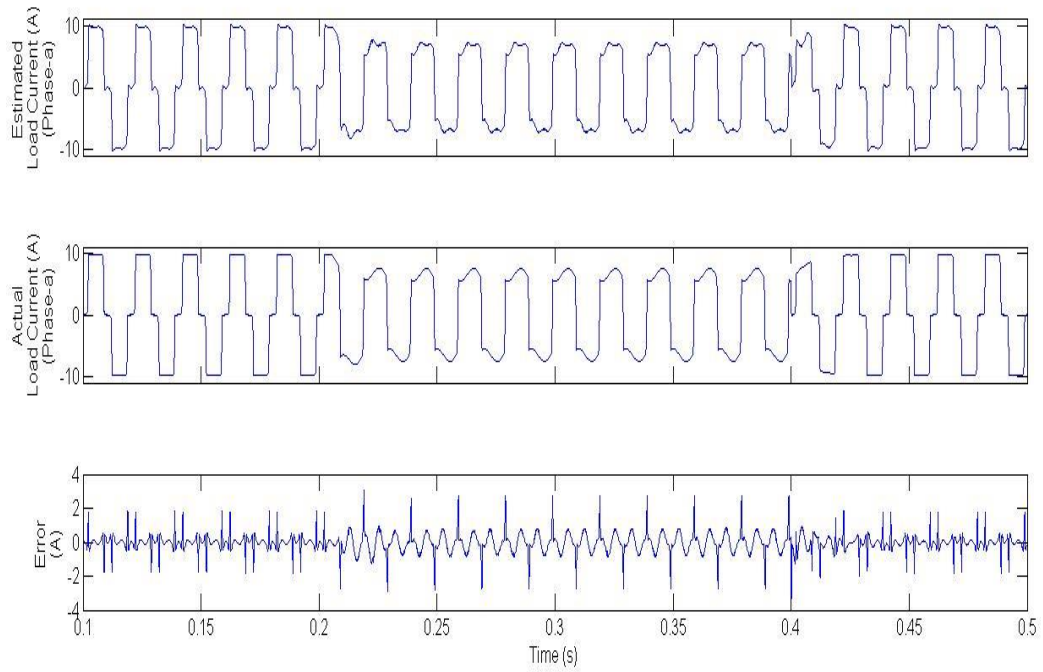

Figure 4.5: Waveforms of estimated load current, actual load current and error.

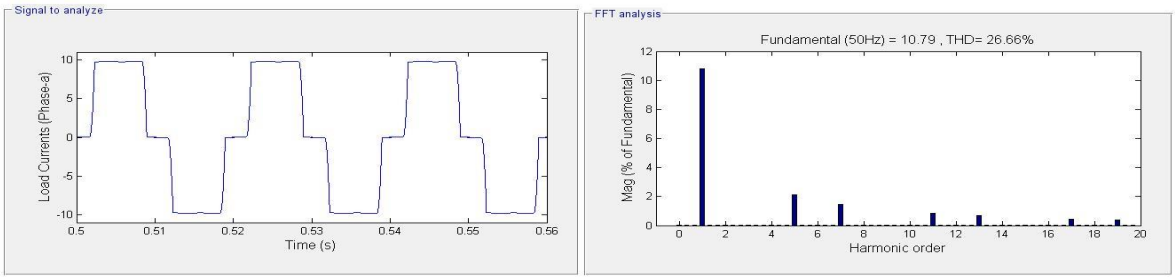

Figure 4.6: FTT analysis is shown for the THD of phase ‘a’ load current.

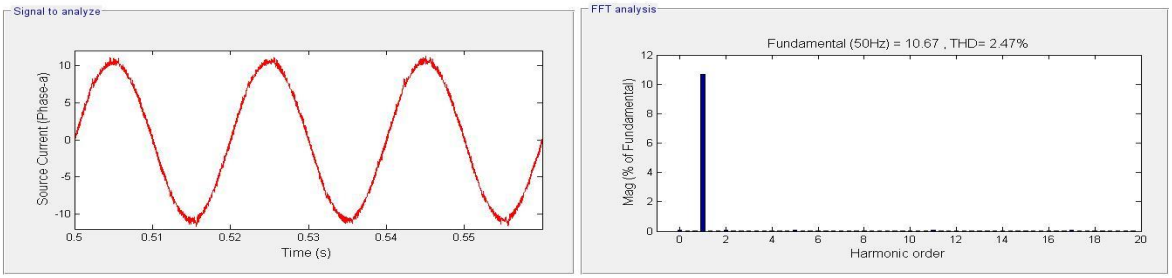

Figure 4.7: FTT analysis is shown for the THD of phase ‘a’ source current.

Figure 4.5 shows the waveforms of estimated load current, actual load current and error. Figure 4.6 and Figure 4.7 show the waveforms and FTT analysis for THD of phase ‘a’ load current and source current. Figure 4.6 shows the THD of phase ‘a’ load current, which is observed as 26.66%. Figure 4.7 shows the THD of phase ‘a’ source current, which is observed as 2.47%.

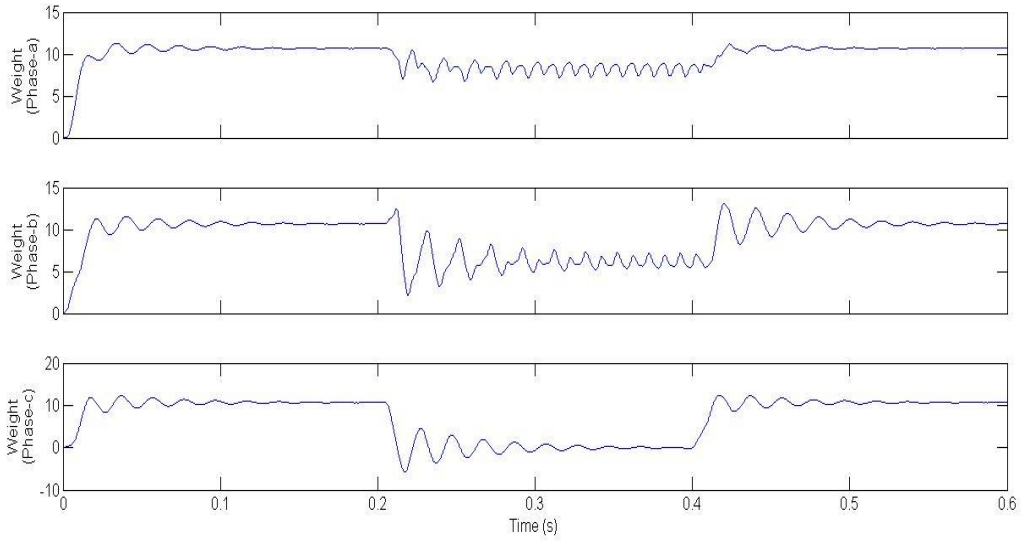

Figure 4.8: Waveforms of the weights of phase ‘a’, ‘b’ and ‘c’.

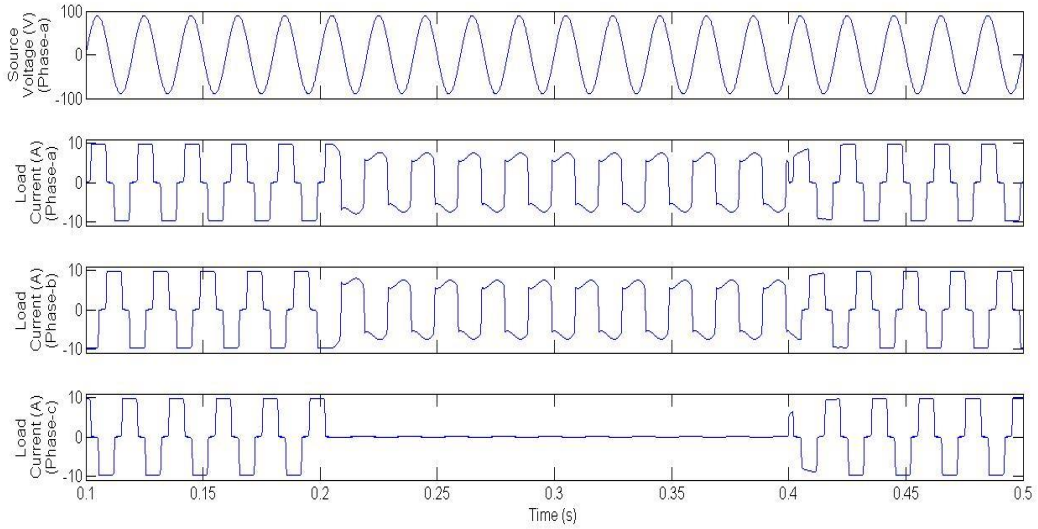

Figure 4.9: Waveforms of phase ‘a’ source voltage with load currents of phase ‘a’, ‘b’ and ‘c’.

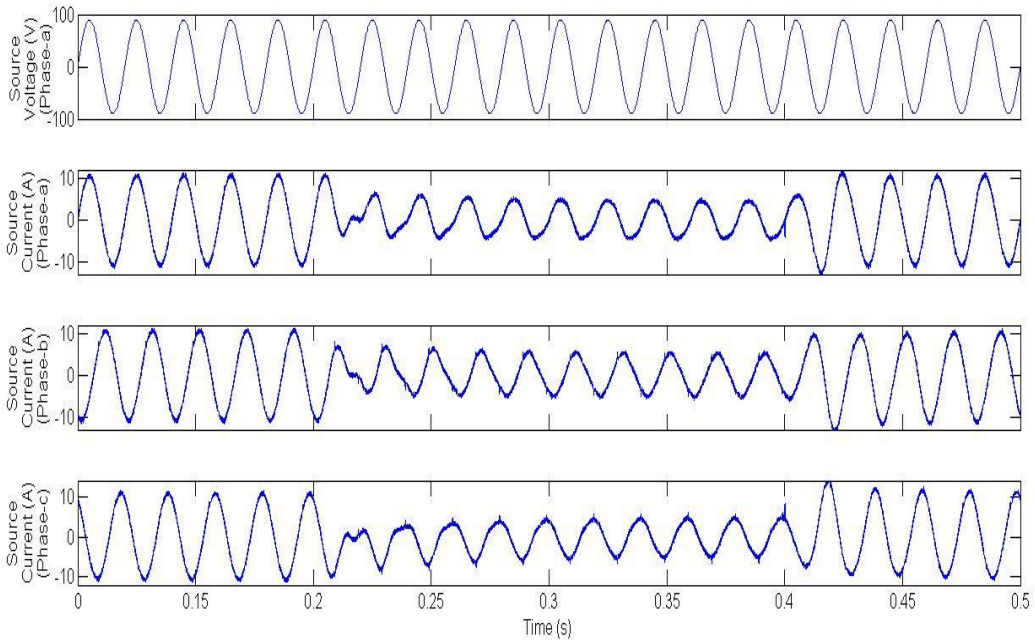

Figure 4.10: Waveforms of phase ‘a’ source voltage with source currents of phase ‘a’, ‘b’ and ‘c’.

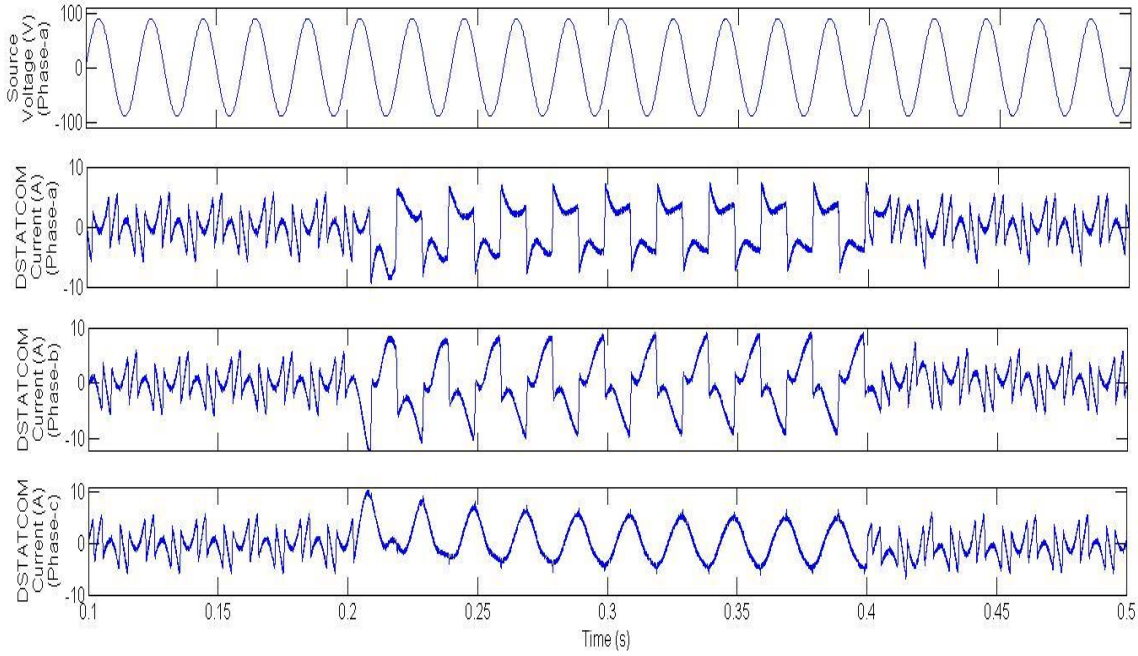

Figure 4.11: Waveforms of phase ‘a’ source voltage with DSTATCOM currents of phase ‘a’, ‘b’ and ‘c’.

Figure 4.8 shows the waveforms of the fundamental weights of the loads currents of phase ‘a’, ‘b’ and ‘c’. Figure 4.9 shows the waveforms of phase ‘a’ source voltage with load currents of phase ‘a’, ‘b’ and ‘c’. Figure 4.10 shows the waveforms of phase ‘a’ source voltage with source currents of phase ‘a’, ‘b’ and ‘c’. Figure 4.11 shows the waveforms of phase ‘a’ source voltage with DSTATCOM currents of phase ‘a’, ‘b’ and ‘c’. In all the waveforms satisfactory results are obtained.

4.4 SIGN-REGRESSOR LMS ALGORITHM

The sign-regressor or data-sign algorithm is given as follows,

$$\mathbf{W}(k+1) = \mathbf{W}(k) + 2\mu e(k)\text{sign}(\mathbf{x}(k)) \tag{4.12}$$

where, the sign function is applied to x(n) on element by element basis.

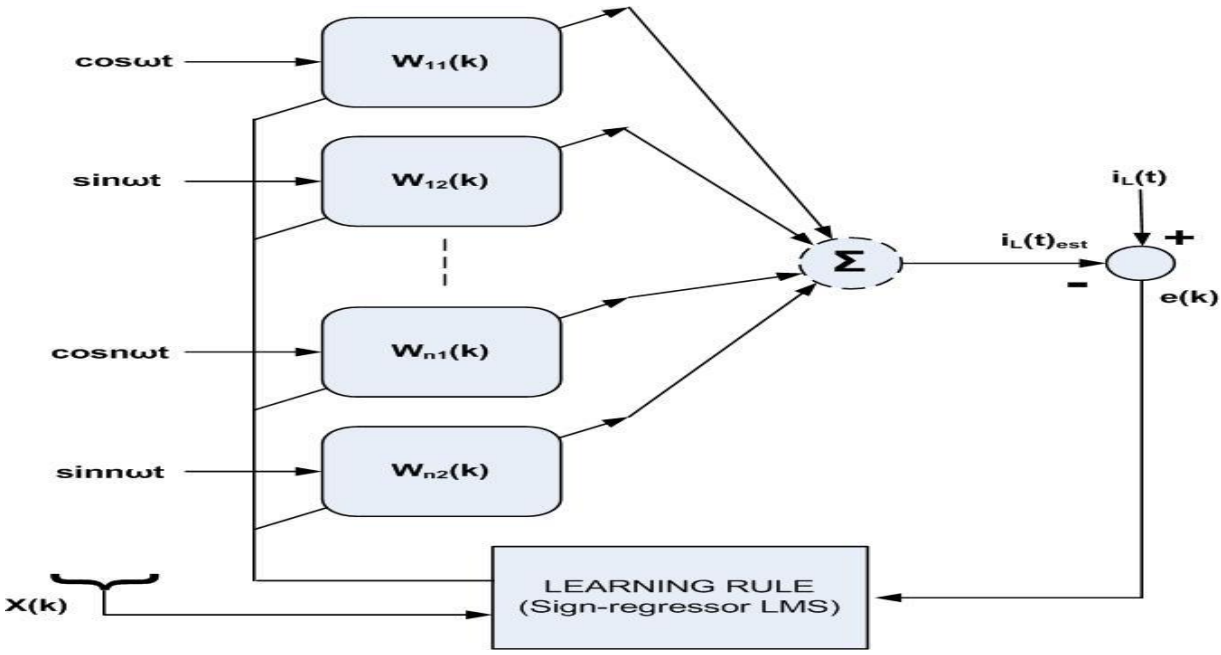

Figure 4.12: Realization of Sign-regressor LMS.

Figure 4.12 shows the realization of adaptive filter based on sign-regressor LMS algorithm for minimizing the error between actual load current and estimated load current. In this scheme, the expression (4.12) is used for the updation of the weights.

4.4.1 SIMULATION RESULTS

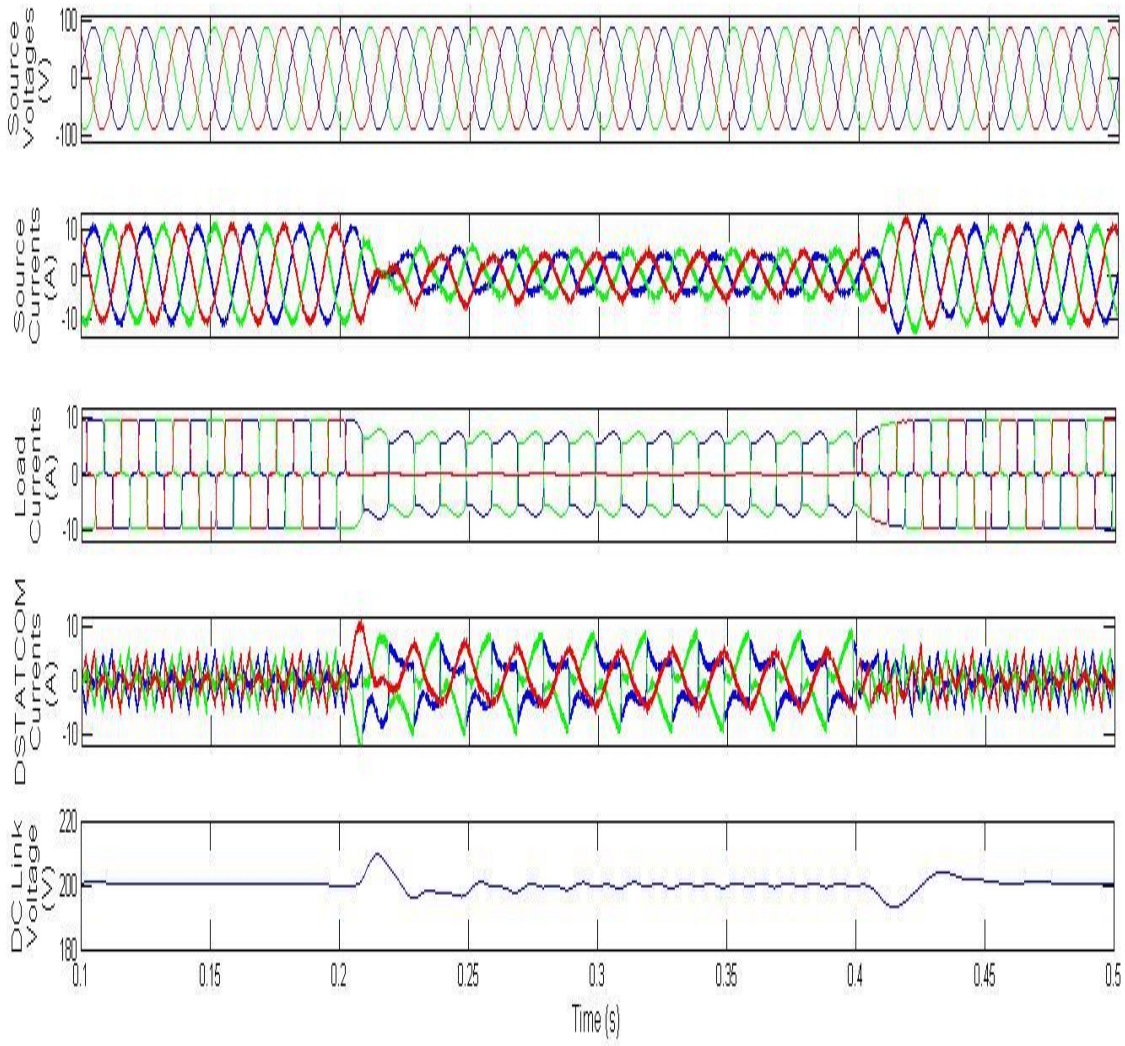

Figure 4.13: Dynamic response of the system is shown with non-linear load condition. Waveforms of source voltages, source currents, load currents, compensator currents and DC link voltage are shown.

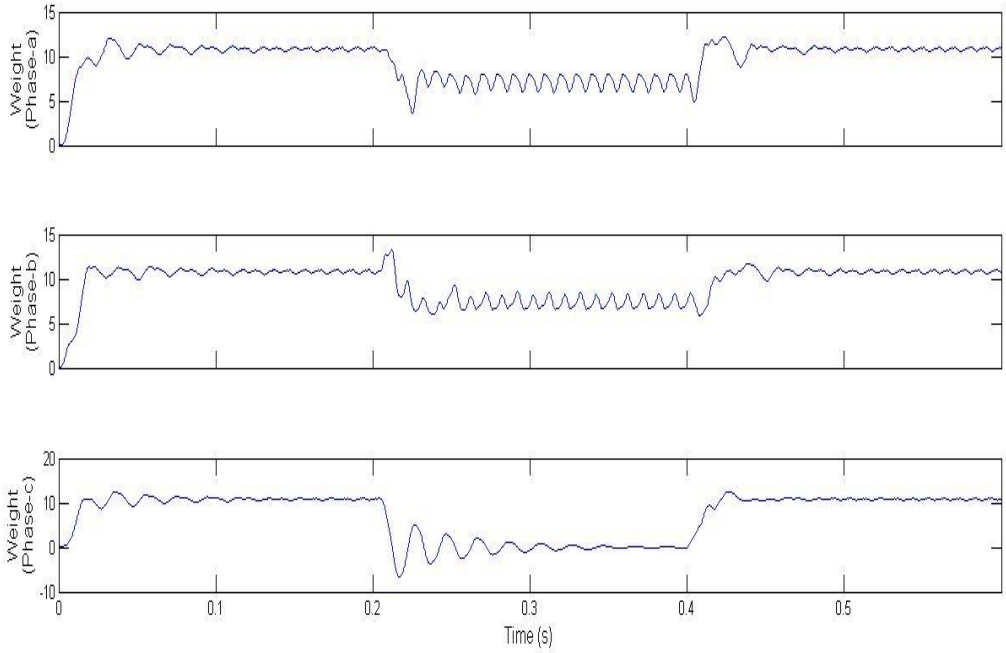

Figure 4.14: Waveforms of the weights of phase ‘a’, ‘b’ and ‘c’.

Figure 4.13 shows the simulation results for the developed system at steady state and unbalanced conditions. In which various plots of supply voltages (V_s), supply currents (i_S), phase ‘a’, ‘b’ & ‘c’ load currents (i_{La}, i_{Lb} & i_{Lc}), compensator currents (i_c) and dc link voltage (V_{dc}). The system is controlled by sign-regressor LMS algorithm based adaptive filter. Till 0.2 the load is balanced and the load currents have THD of 26.23% with the implementation of DSTATCOM the dc link is maintain to 200V and the supply currents are observed to balanced and sinusoidal. The THD of supply current is 2.42% in steady state condition. The unbalancing (load removal) is done in phase ‘c’ in DSTATCOM to the load side at 0.2 sec for interval of 0.2 sec and at 0.4 sec the load is reconnected. It can be seen that the waveforms of source currents are sinusoidal during balance loading as well as unbalance loading. Figure 4.14 shows the waveforms of the fundamental weights of load currents of phase ‘a’, ‘b’ and ‘c’. In which, it can be seen that the fundamental weights are settled down to their corresponding amplitudes of phase current.

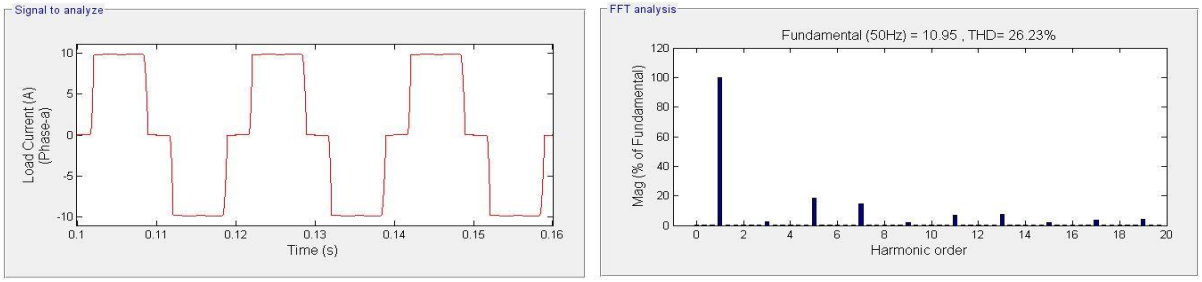

Figure 4.15: FTT analysis is shown for the THD of phase ‘a’ load current.

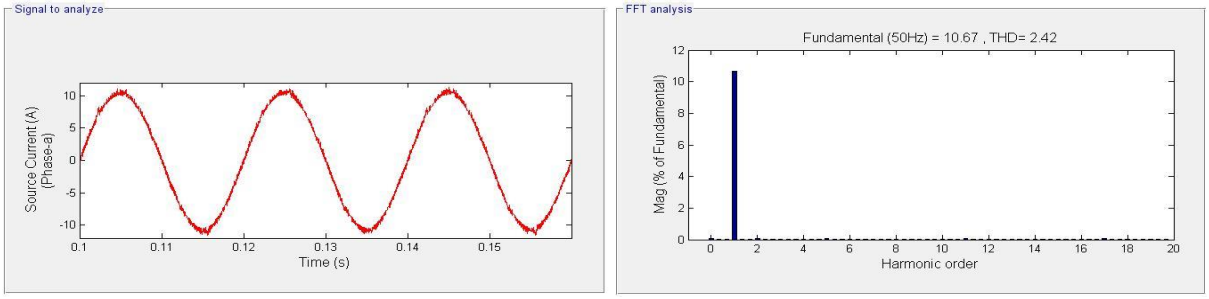

Figure 4.16: FTT analysis is shown for the THD of phase ‘a’ source current.

Figure 4.15 and Figure 4.16 show the waveforms and FTT analysis for THD of phase ‘a’ load current and source current. Figure 4.15 shows the THD of phase ‘a’ load current, which is observed as 26.23%. Figure 4.16 shows the THD of phase ‘a’ source current, which is observed as 2.42%.

4.5 NORMALIZED LMS ALGORITHM

For the decomposition of weights corresponding to the all components of load currents, the adalines are adopted with the help of Normalized LMS learning rule written as follows.

$$\mathbf{W}(k+1) = \mathbf{W}(k) + \frac{1}{x^T(k)x(k)}e(k)\mathbf{x}(k) \quad (4.13)$$

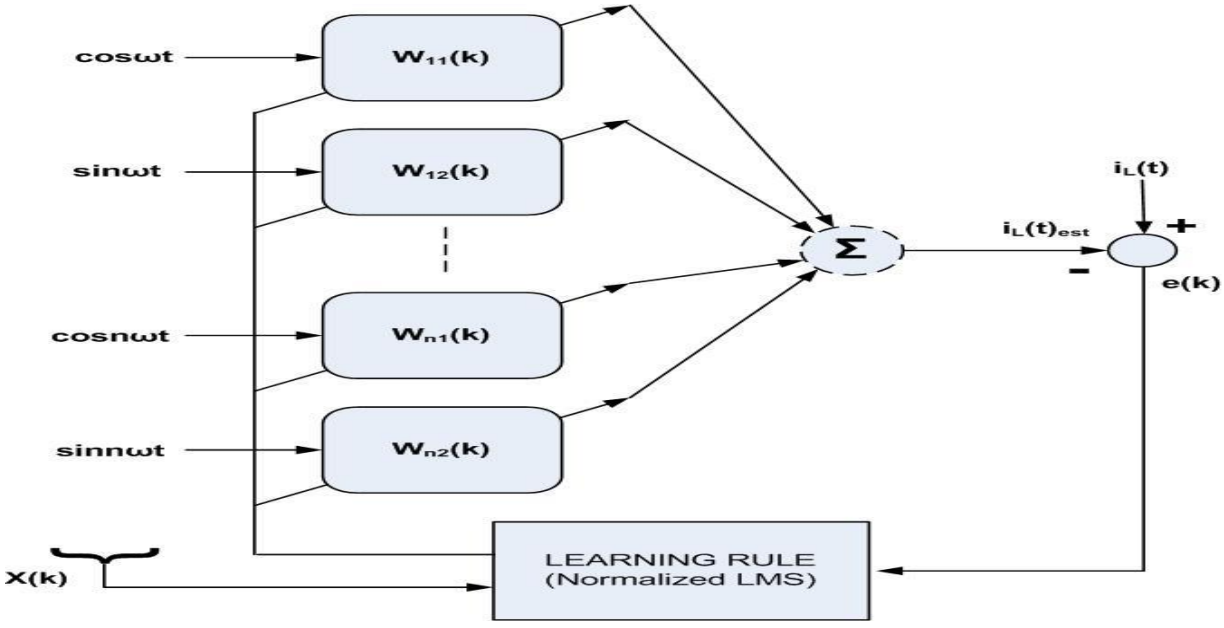

Figure 4.17: Realization of normalized LMS.

Figure 4.17 shows the realization of adaptive filter based on normalized LMS algorithm for minimizing the error between actual load current and estimated load current.

4.5.1 SIMULATION RESULTS

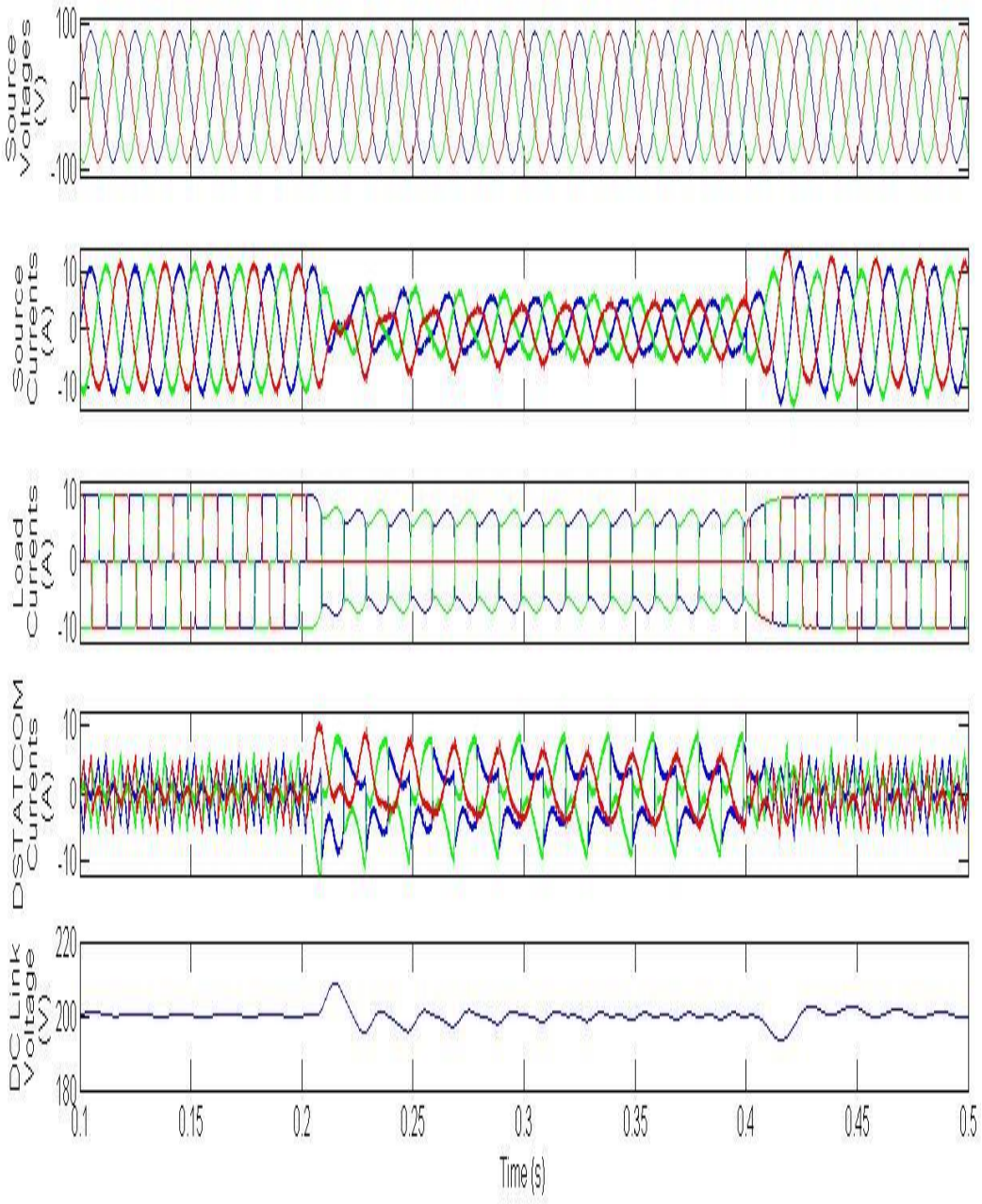

Figure 4.18: Dynamic response of the system is shown with non-linear load condition. Waveforms of source voltages, source currents, load currents, compensator currents and DC link voltage are shown.

Figure 4.18 shows the simulation results for the developed system at steady state and unbalanced conditions. In which various plots of supply voltages (V_s), supply currents (i_S), phase 'a', 'b' & 'c' load currents (i_{La}, i_{Lb} & i_{Lc}), compensator currents (i_c) and dc link voltage (V_{dc}). The system is controlled by normalized LMS algorithm based adaptive filter. Till 0.2 the load is balanced and the load currents have THD of 27.13% with the implementation of DSTATCOM the dc link is maintain to 200V and the supply currents are observed to balanced and sinusoidal. The THD of supply current is 2.63% in steady state condition. The unbalancing (load removal) is done in phase 'c' in DSTATCOM to the load side at 0.2 sec for interval of 0.2 sec and at 0.4 sec the load is reconnected. It can be seen that the waveforms of source currents are sinusoidal during balance loading as well as unbalance loading. Figure 4.19 shows the waveforms of the fundamental weights of load currents of phase 'a', 'b' and 'c'. In which, it can be seen that the fundamental weights are settled down to their corresponding amplitudes of phase current.

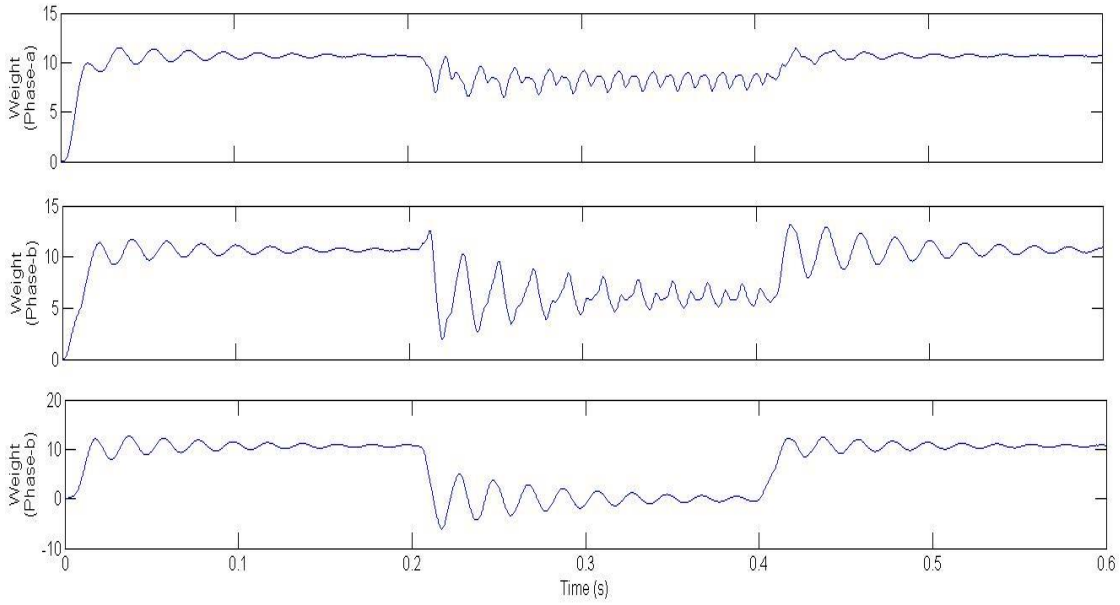

Figure 4.19: Waveforms of the weights of phase 'a', 'b' and 'c'.

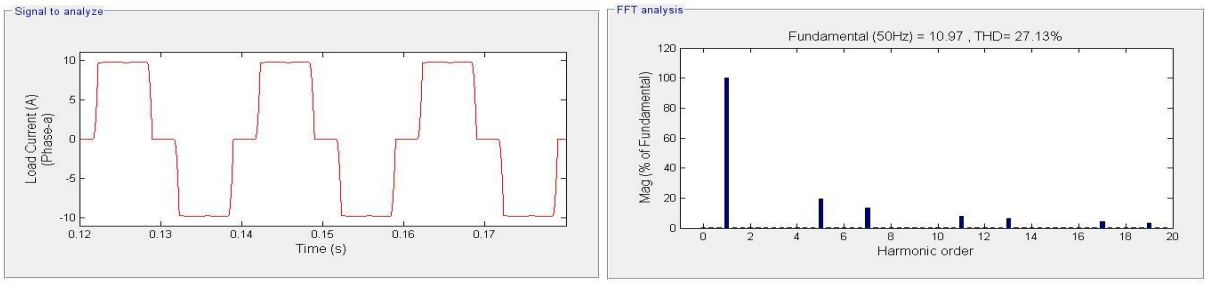

Figure 4.20: FTT analysis is shown for the THD of phase ‘a’ load current.

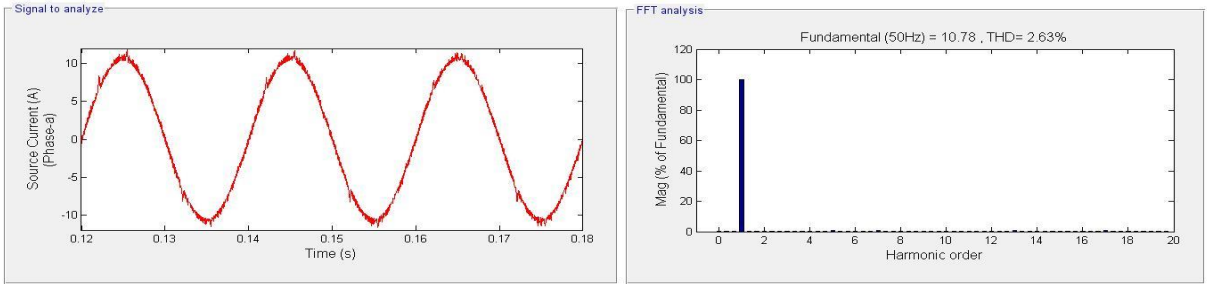

Figure 4.21: FTT analysis is shown for the THD of phase ‘a’ source current.

Figure 4.20 and Figure 4.21 show the waveforms and FTT analysis for THD of phase ‘a’ load current and source current. Figure 4.20 shows the THD of phase ‘a’ load current, which is observed as 27.13%. Figure 4.21 shows the THD of phase ‘a’ source current, which is observed as 2.63%.

4.6 COMPARISONS

Satisfactory results are obtained from the all the three LMS algorithms i.e. Simple LMS, Sign-regressor LMS and Normalized LMS. Table 4.1 contains THD in source and load current of the three schemes.

Table 4.1: A comparison list of THD in source current and load current

Algorithm	THD in Source current (%)	THD in Load current (%)
Simple LMS	2.47	26.66
Sign-regressor LMS	2.42	26.23
Normalized LMS	2.63	27.13

4.7 CONCLUSION

Adaptive filtering with three LMS based techniques have been studied and simulations in Simulink/MATLAB have been done. Results are compared of all three controllers. The three techniques are Simple LMS Algorithm, Sign-regressor LMS Algorithm and Normalized LMS Algorithm. As the comparison in Table 4.1 shows, Simple LMS gives THD of source current 2.47%, Sign-regressor LMS gives THD 2.42% and Normalized LMS gives THD 2.63%. All the schemes work equally well.

CHAPTER 5

ADAPTIVE WIENER FILTER

5.1 GENERAL

In this chapter, adaptive Wiener filter is discussed. Steepest descent method is used for the updation the tap weights corresponding to the amplitude of the different harmonic components of load current.

5.2 WIENER FILTER

Wiener filter is a class of linear optimum discrete-time filter. These filters are optimum in the sense of minimizing an appropriate function of the error, known as the cost function [29, 30]. The cost function that is commonly used in filter design optimization is the mean-square error (MSE). [42-46]

Let the sample response (filter coefficients) of the Wiener filter be denoted by W. This filter will process the real valued stationary process {x(k)} to produce an estimate $\hat{d}(k)$ of the desired real valued signal d(k). It is assumed that the processes {x(k)}, {d(k)}, etc., have zero mean values. Furthermore, assuming that the filter coefficients do not change with time, the output of the filter is equal to the convolution of the input and the filter coefficients. Hence we obtain

$$\hat{d}(k) = \sum_{m=0}^{M-1} W_m x(k-m) = \mathbf{W^T x}(k) \tag{5.1}$$

where, M is the number of filter coefficients, and

$$\mathbf{W} = [W_1\ W_2\ \ldots\ldots\ W_{M-1}]^T,\ \mathbf{x}(k) = [x(k)\ x(k-1)\ x(k-2)\ \ldots\ldots\ x(k-M+1)]^T \tag{5.2}$$

The MSE function (cost function) is given by

$$J(\mathbf{W}) = E\{e^2(k)\} = E\{[d(k) - \mathbf{W^T x}(k)]^2\}$$

$$= E\{[d(k) - \mathbf{W^T x}(k)]\ [d(k) - \mathbf{W^T x}(k)]^T\}$$

$$= E\{[d^2(k) - \mathbf{W^T x}(k)d(k) - d(k)\mathbf{x^T}(k)\mathbf{W} + \mathbf{W^T x}(k)\mathbf{x^T}(k)\mathbf{W}]\}$$

$$= E\{d^2(k)\} - 2\mathbf{W}^T E\{ d(k)\mathbf{x}(k)\} + \mathbf{W}^T E\{\mathbf{x}(k)\, \mathbf{x}^T(k)\}\mathbf{W}$$

$$= \sigma^2_d - 2\mathbf{W}^T\mathbf{p}_{dx} + \mathbf{W}^T\mathbf{R}_x\mathbf{W} \quad (5.3)$$

where,

$\mathbf{W}^T\mathbf{x}(k) = \mathbf{x}^T(k)\mathbf{W}$ = scalar

σ^2_d = variance of the desired signal, d(k)

$$\mathbf{p}_{dx} = [p_{dx}(0)\ p_{dx}(1)\ \ldots\ldots\ p_{dx}(M-1)]^T \quad (5.4)$$

= cross-correlation vector between d(k) and $\mathbf{x}(k)$

$$\mathbf{R}_x = E\{\mathbf{x}(k)\, \mathbf{x}^T(k)\} \quad (5.5)$$

$\mathbf{R}_x$ is the correlation matrix of the input data and it is symmetric because the random process is assumed to be stationary and hence we have equality, $r_x(k) = r_x(-k)$.

To find the minimum value of the MSE surface, here steepest descent algorithm is used for updating weights as follows,

a) We start with the initial value $\mathbf{W}(0)$, we compute the gradient vector.
b) At the MSE surface point that corresponds to $\mathbf{W}(0)$, we compute the gradient vector $\Delta J(\mathbf{W}(0))$.
c) We compute the value $-\mu\Delta J(\mathbf{W}(0))$ and add it to $\mathbf{W}(0)$ to obtain $\mathbf{W}(1)$.
d) We go back to step b) and continue the procedure until we find the optimum value of the vector coefficients.

If $\mathbf{W}(k)$ is the filter-coefficient vector at step k (time), then its updated value $\mathbf{W}(k+1)$ is given by

$$\mathbf{W}(k+1) = \mathbf{W}(k) - \mu\Delta J(\mathbf{W}(0)) \quad (5.6)$$

The gradient vector is equal to

$$\Delta J(\mathbf{W}(k)) = -2\,\mathbf{p}_{dx} + 2\mathbf{R}_x\mathbf{W}(k) \quad (5.7)$$

and hence equation (5.6) becomes

$$\mathbf{W}(k+1) = \mathbf{W}(k) + 2\mu[\mathbf{p}_{dx} - \mathbf{R}_x\mathbf{W}(k)] \quad (5.8)$$

where, μ is the value of step size parameter and this is to be kept less than 0.5.

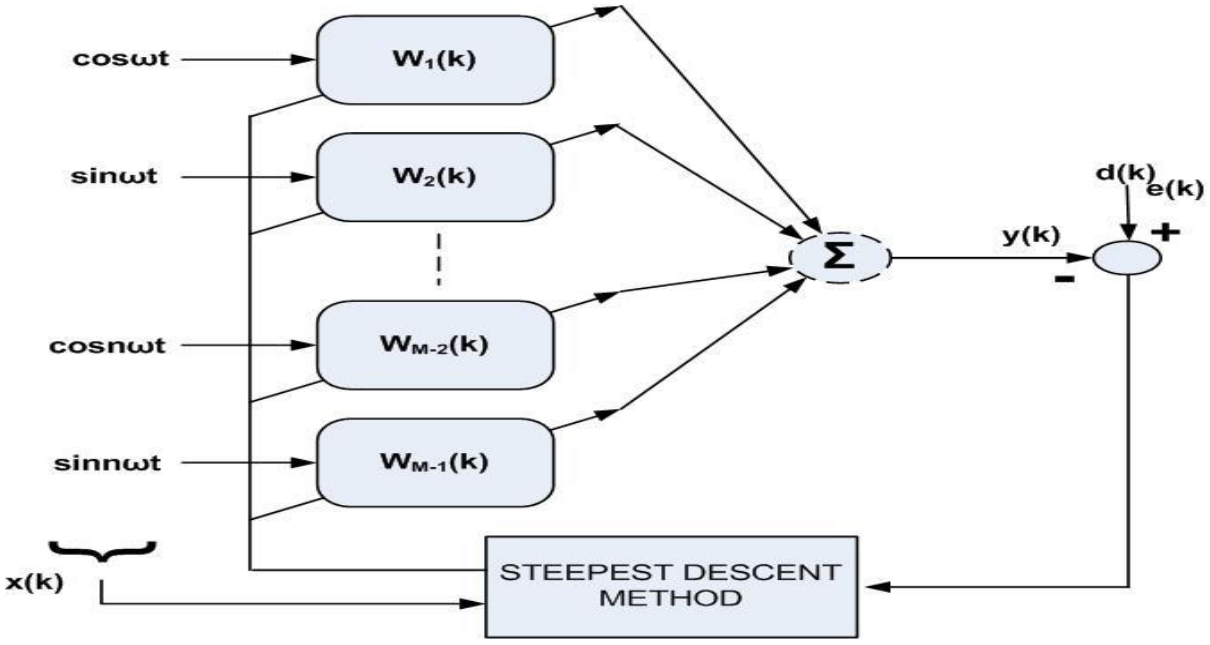

Figure 5.1: Realization of Wiener Filter.

Figure 5.1 shows the diagram of Adaptive filter based on Weiner filtering scheme, in which Steepest Descent method is used for the weight updation.

5.3 SIMULATION RESULTS

Figure 5.2 shows the simulation results for the developed system at steady state and unbalanced conditions. In which various plots of supply voltages (V_s), supply currents (i_S), phase 'a', 'b' & 'c' load currents (i_{La}, i_{Lb} & i_{Lc}), compensator currents (i_c) and dc link voltage (V_{dc}). The system is controlled by Wiener filtering scheme. Till 0.3 the load is balanced and the load currents have THD of 26.63% with the implementation of DSTATCOM the dc link is maintain to 200V and the supply currents are observed to balanced and sinusoidal. The THD of supply current is 2.64% in steady state condition. The unbalancing (load removal) is done in phase 'c' in DSTATCOM to the load side at 0.3 sec for interval of 0.2 sec and at 0.5 sec the load is reconnected. It can be seen that the waveforms of source currents are sinusoidal during

balance loading as well as unbalance loading. Figure 5.3 shows the waveforms of the fundamental weights of load currents of phase ‘a’, ‘b’ and ‘c’.

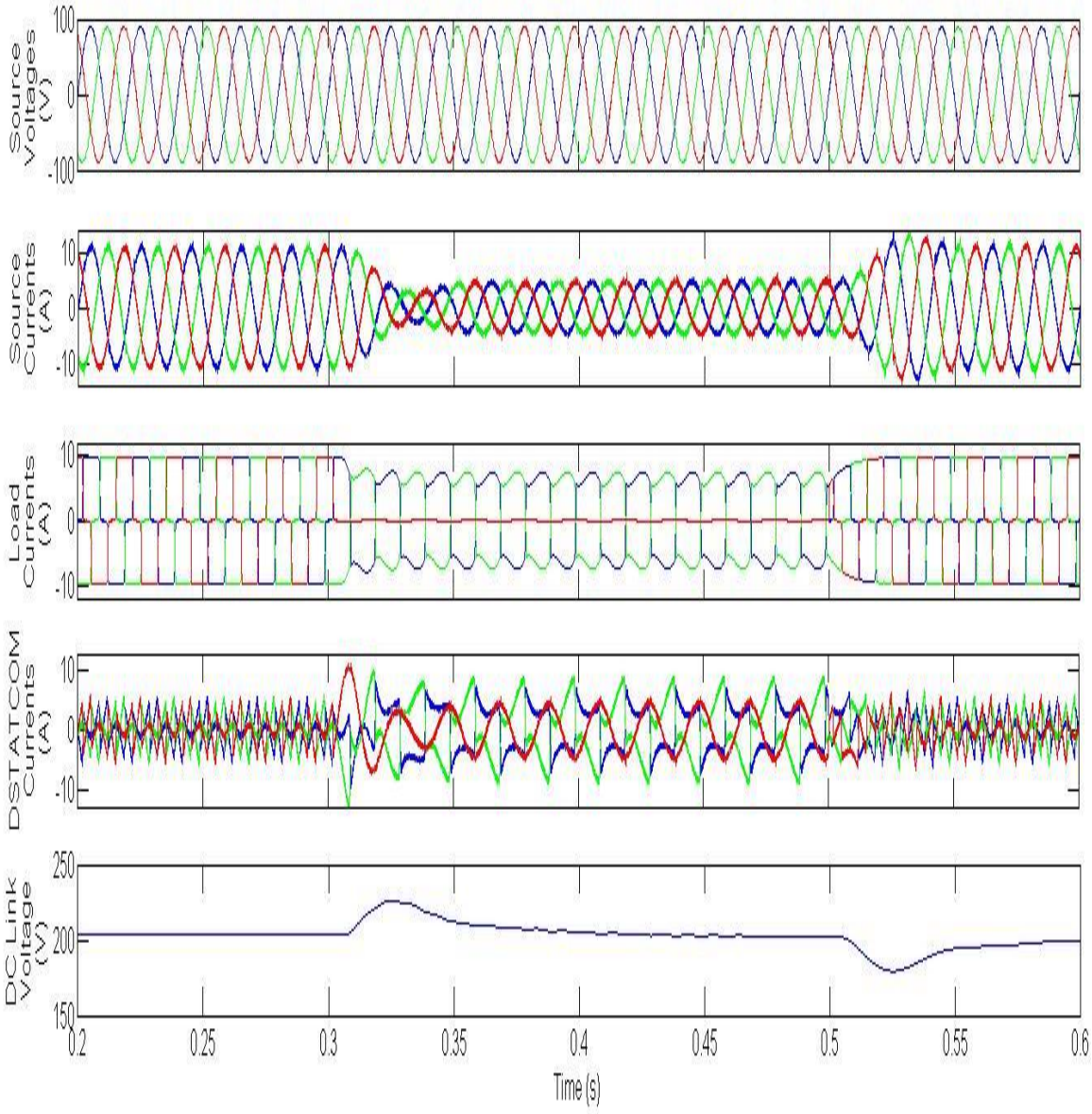

Figure 5.2: Dynamic response of the system is shown with non-linear load condition. Waveforms of source voltages, source currents, load currents, compensator currents and DC link voltage are shown.

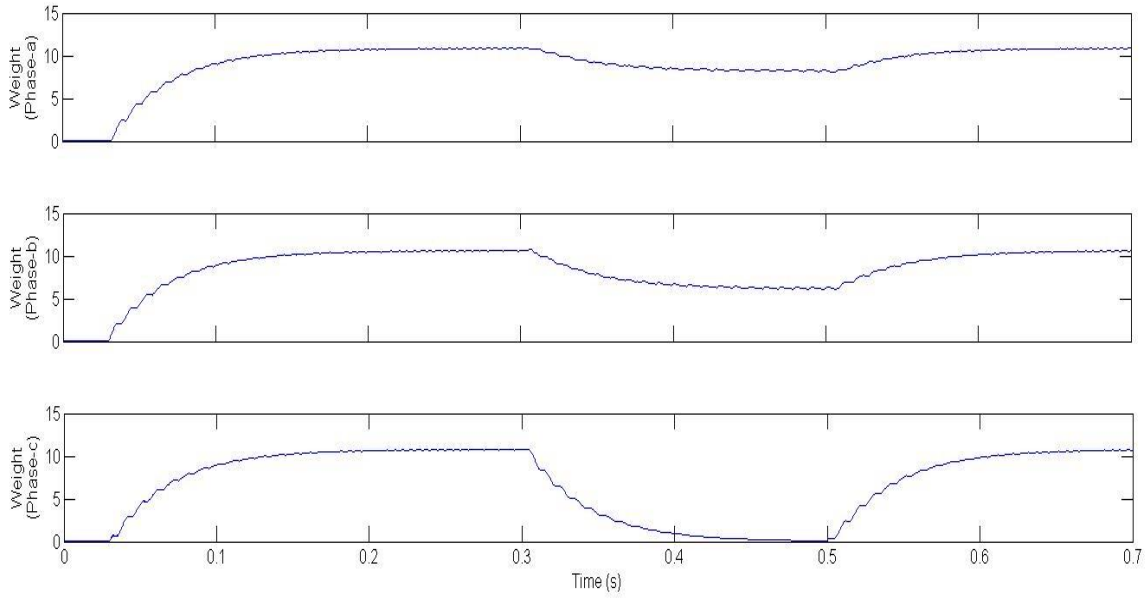

Figure 5.3: Waveforms of the weights of phase ‘a’, ‘b’ and ‘c’.

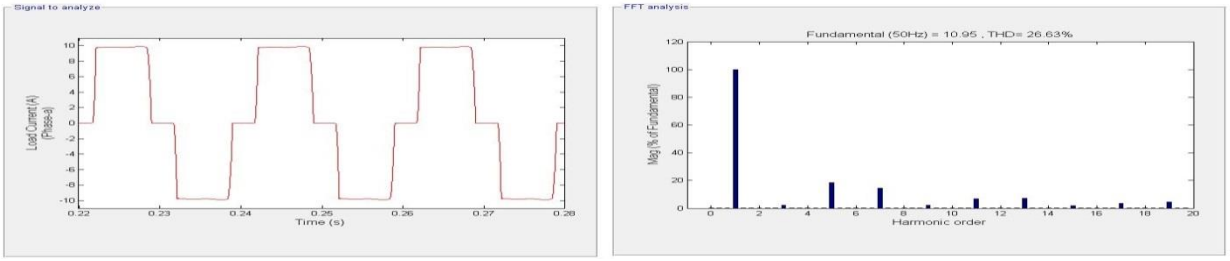

Figure 5.4: FTT analysis is shown for the THD of phase ‘a’ load current.

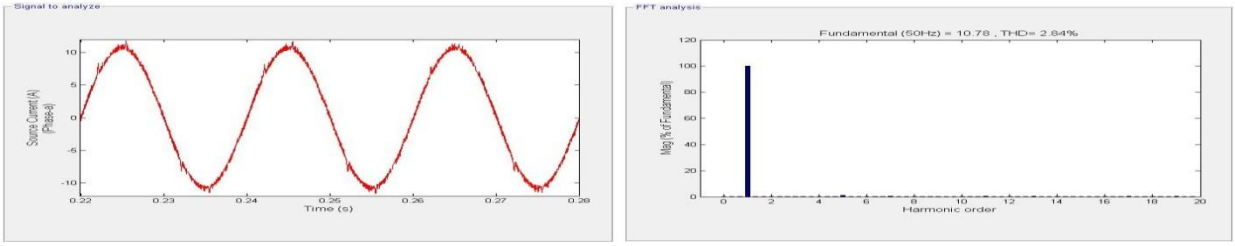

Figure 5.5: FTT analysis is shown for the THD of phase ‘a’ source current.

Figure 5.4 and Figure 5.5 show the waveforms and FTT analysis for THD of phase ‘a’ load current and source current. Figure 5.4 shows the THD of phase ‘a’ load current, which is observed as 26.63%. Figure 5.5 shows the THD of phase ‘a’ source current, which is observed as 2.64%.

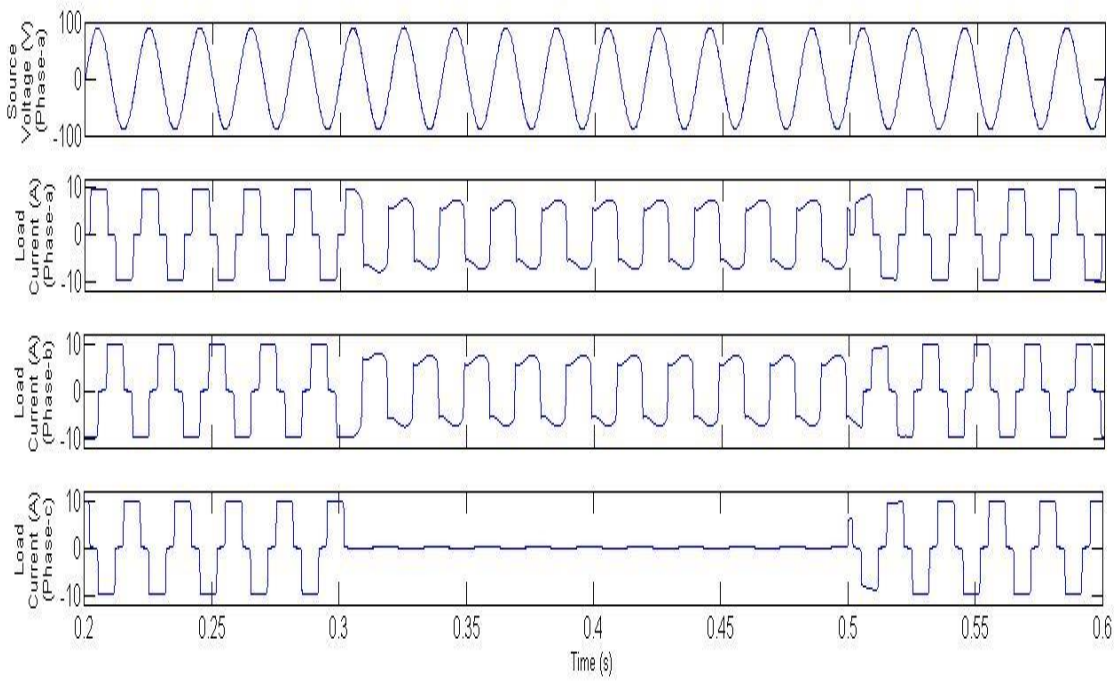

Figure 5.6: Waveforms of phase 'a' source voltage with load currents of phase 'a', 'b' and 'c'.

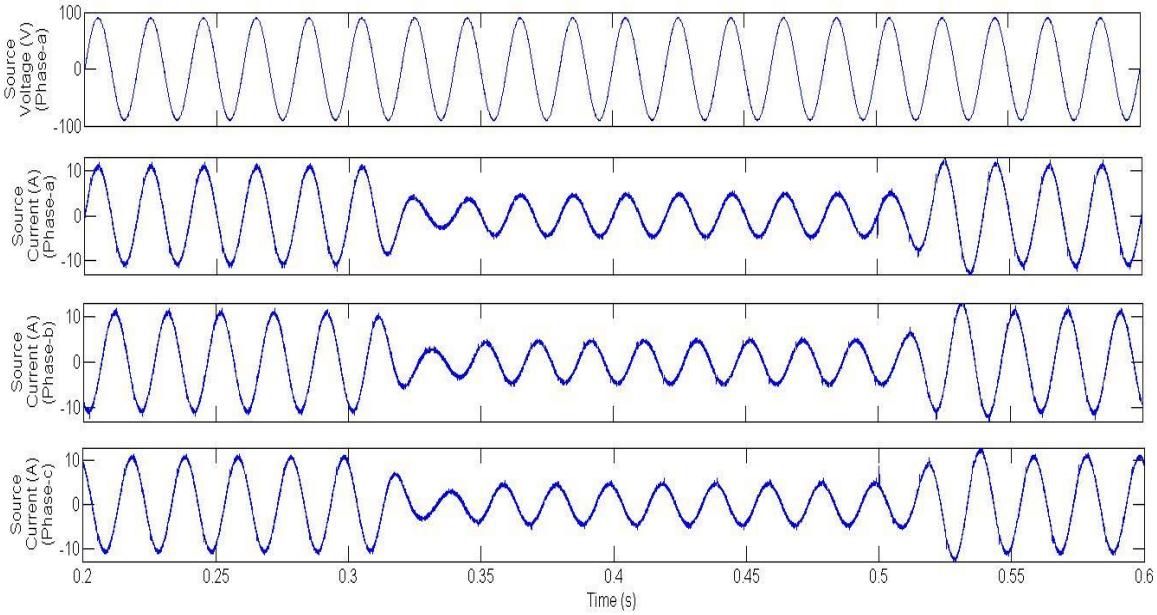

Figure 5.7: Waveforms of phase 'a' source voltage with source currents of phase 'a', 'b' and 'c'.

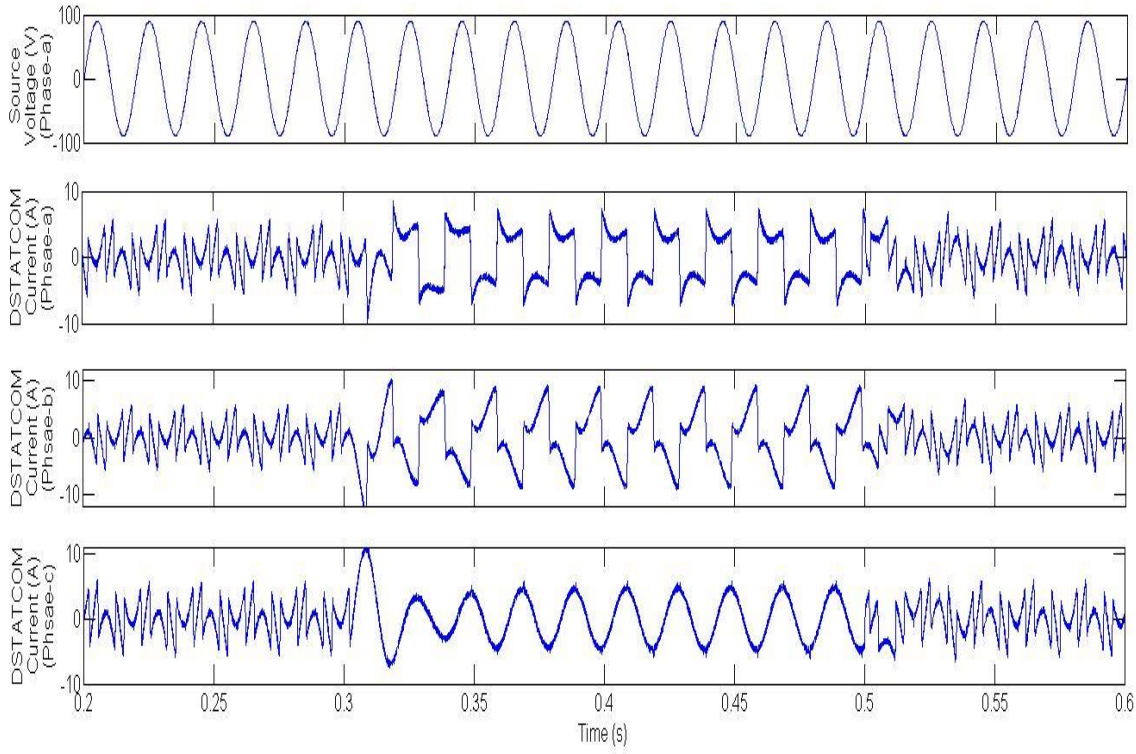

Figure 5.8: Waveforms of phase ‘a’ source voltage with DSTATCOM currents of phase ‘a’, ‘b’ and ‘c’.

Figure 5.6 shows the waveforms of phase ‘a’ source voltage with load currents of phase ‘a’, ‘b’ and ‘c’. Figure 5.7 shows the waveforms of phase ‘a’ source voltage with source currents of phase ‘a’, ‘b’ and ‘c’. Figure 5.8 shows the waveforms of phase ‘a’ source voltage with DSTATCOM currents of phase ‘a’, ‘b’ and ‘c’. In all the waveforms satisfactory results are obtained.

5.4 HARDWARE RESULTS

Figure 5.9 to Figure 5.15 show the hardware implemented results of the proposed system for compensating the harmonics with non-linear load in balanced and unbalanced conditions, which are shown on three phase power analyzer (Fluke model 434, series-II Energy Analyzer).

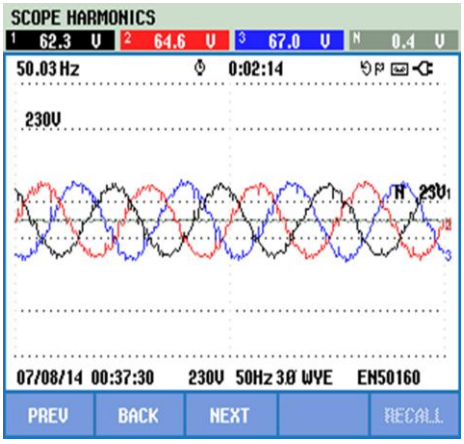

Figure 5.9: Waveforms of source voltages.

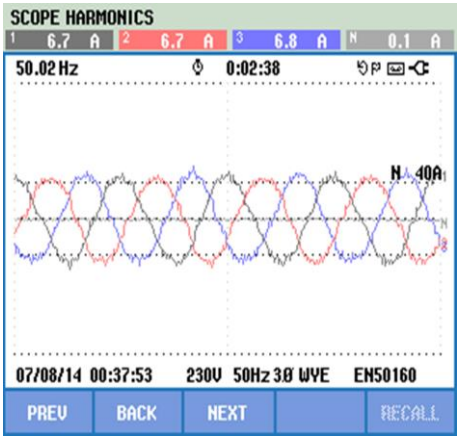

Figure 5.10: Waveforms of source currents.

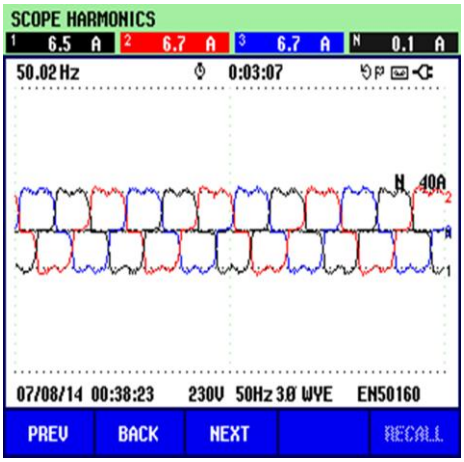

Figure 5.11: Waveforms of load currents.

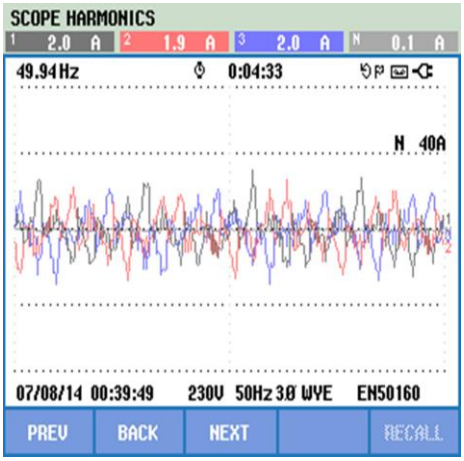

Figure 5.12: Waveforms of DSTACOM currents.

Figure 5.9 to Figure 5.12 show the waveforms of the voltages and currents. Figure 5.9 shows the three phase voltage waveforms of the source, which are sinusoidal. Figure 5.10 shows the waveforms of the three phase source currents, which are also sinusoidal after the compensation. Figure 5.11 shows the waveforms of the three phase load currents, which are much distorted from the sinusoidal waveform as shown in figure. Figure 5.12 shows the waveforms of the three phase DSTATCOM currents and it can be observed that these currents are highly distorted to compensate the harmonics of the load currents.

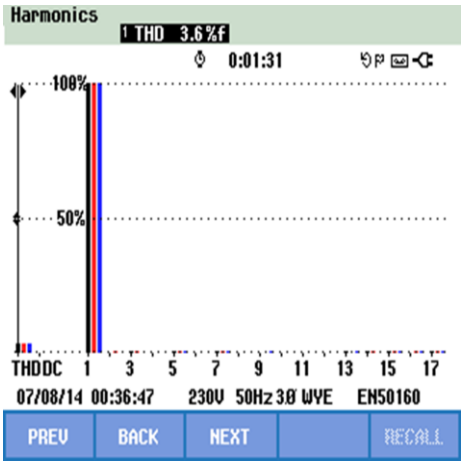

Figure 5.13: THD in source voltages.

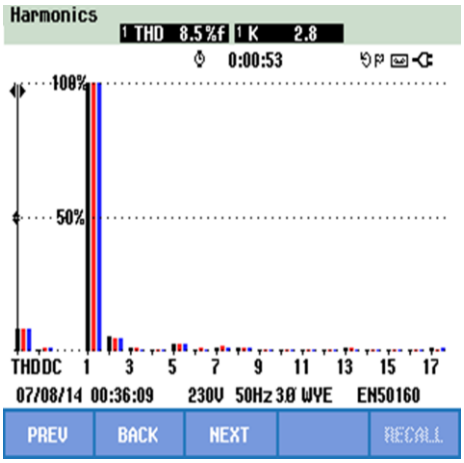

Figure 5.14: THD in source currents.

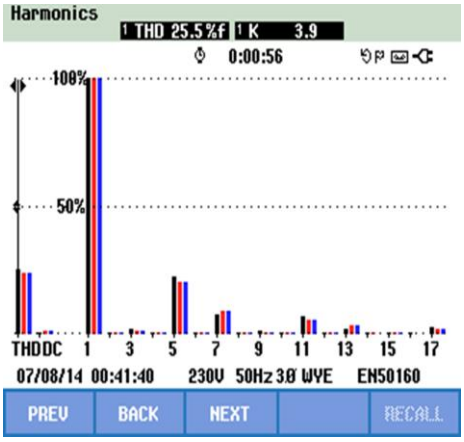

Figure 5.15: THD in load currents.

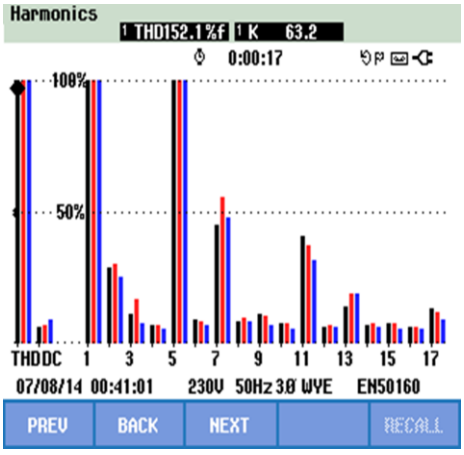

Figure 5.16: THD in DSTATCOM currents.

Figure 5.13 to Figure 5.16 show the THD percentage of the voltages and currents waveforms. Figure 5.13 shows the THD of the source voltages, which is observed as 3.6%. Figure 5.14 shows the THD of the source currents, which is observed as 8.5%. Figure 5.15 shows the THD of the load currents, which is observed as 25.5%. Figure 5.16 shows the THD of the DSTATCOM currents, which is observed as 152.1%. It can be observed that the THD of source currents is reduced from 25.5% (in case of without compensation) to 8.5% (after compensation).

5.5 CONCLUSION

Simulations and hardware implementations of the adaptive Wiener filter are simulated and implemented. On comparing this filter response with the LMS based filters of previous chapters, it is observed that Wiener filter based scheme is better able to extract the fundamental component of load current. Its computation is faster than LMS schemes.

CHAPTER 6

CONCLUSIONS AND FUTURE SCOPE

6.1 CONCLUSIONS

In this work, the energy scenario of the world and India in particular has been discussed. A typical power distribution structure layout is explained at generation, transmission, sub-transmission and distribution level. Power quality problems and Custom power devices i.e. DSTATCOM, DVR and UPQC are discussed. Operation modes, parameters and controlling of DSTATCOM are studied.

Literature survey related to the work has been done in many fields related to power system. Mainly power quality problems, possible solutions, custom power devices, many controllers based on different algorithms. Some algorithms like Fryze current minimization algorithm, Adaptive filtering based on LMS and Wiener filtering scheme have been studied. The proposed system is described in detail with all required parameters.

Hardware implementation of prototype DSTATCOM is implemented and realized with generalized Fryze current minimization control strategy with non-linear loads and it is observed that power quality of the system is improved satisfactorily. Reference currents are extracted by sensing the load currents from current sensors by conductance formula. The switching signals for the gate of IGBTs are derived from HCC. The voltage of dc capacitor is maintained by the help of PI controller in all the cases. The conductance based Fryze control scheme is found to be very effective in reducing the THD within 5% of supply current as per the IEEE-519 standards.

Adaptive filtering with three LMS rules (simple LMS, Sign-regressor LMS and Normalized LMS) has been studied and simulations in Simulink/MATLAB have been done. Results are compared of all three controllers.

Simulations and hardware implementations of the adaptive wiener filter are simulated and implemented. Moreover, the all schemes work well under dynamics of load changes, load unbalancing and removal of load too.

6.2 FUTURE SCOPE OF WORK

1. There are many conventional control algorithms like IRPT, SRF etc. as well as many other adaptive filtering control algorithms cab be implemented. There are many adaptive filtering control algorithms such as normalized LMS sign algorithm, sign-sign LMS algorithm, variable step size LMS (VSLMS) algorithm, the leaky LMS algorithm, linearly constrained LMS algorithm, Kalman filtering algorithm, self-correcting adaptive filtering (SCAF), transform domain adaptive LMS filtering, recursive least-squares (RLS) algorithms, QR-RLS algorithms etc. can be implemented.

2. The proposed system is capable of harmonic compensation as well as reactive power compensation for the distribution system, but it is unable to transfer the active power to the distribution system, because there is no active power source at the DSTATCOM side. So one improvement can be in the system by making the system capable to transfer the active power in the distribution system by adding any real power source such as battery energy storage system (BESS) or renewable source (wind power system, solar power system etc.).

3. For maintaining the DC link voltage, the DC voltage regulator with PI-controller can be replaced by using controller based on Artificial neural network (ANN), Fuzzy algorithm, Particle swarm optimization (PSO) technique, ANFIS (Adaptive Neuro Fuzzy Inference System) and many more optimization techniques.

REFERENCES

[1] http://www.mecometer.com/topic/electricity-installed-generating-capacity.

[2] http://www.cea.nic.in/reports/monthly/inst_capacity/dec13.pdf, ministry of power, Central electricity authority, government of India.

[3] http://www.powermin.nic.in/indian_electricity_scenario/introduction.htm, ministry of power, government of India.

[4] http://www.mnre.gov.in/mission-and-vision-2/achievements/, Ministry Of New And Renewable Energy, Government of India.

[5] Arindam Ghosh and Gerard Ledwich, "Power Quality Enhancement Using Custom Power Devices", Kluwer Academic Publishers, 101 Philip Drive, Assinippi Park, Norwell, Massachusetts 02061 USA.

[6] D.P. Kothari and I.J. Nagrath, Power System Engineering, 2nd edition, Tata McGraw-Hill, New Delhi, 2008.

[7] Sunil S. Rao, Switchgear, Protection and Power Systems, 13th edition, Khanna Publisher, New Delhi, 2008.

[8] R. Sastry Vedam, Mulukutla S. Sarma, POWER QUALITY, VAR Compensation in Power Systems, CRC Press Taylor & Francis Group, 6000 Broken Sound Parkway NW, Suite 300, Boca Raton, FL 33487-2742.

[9] Roger C. Dugan, Mark F. McGranaghan, Surya Santoso, H. Wayne Beaty, Electrical Power System Quality, 2nd edition, The McGraw-Hill Companies, 2004.

[10] Ravilla Madhusudan, G. Ramamohan Rao, "Modeling and Simulation of a Distribution STATCOM (D-STATCOM) for Power Quality Problems-Voltage Sag and Swell Based on Sinusoidal Pulse Width Modulation (SPWM)", IEEE- International Conference On Advances In Engineering, Science And Management (ICAESM -2012) March 30, 31, 2012.

[11] Pudi Sekhar, K. Venkateswara Rao and T.Devaraju, "Power Quality Enhancement using Custom Power Devices", International Electrical Engineering Journal (IEEJ) Vol. 3 (2012) No. 2, pp. 745-750.

[12] Parmar Hiren.S, Vamsi Krishna.K, Ranjit Roy, "Shunt Compensation for Power Quality Improvement using a STATCOM Controller" Proc. of Int. Conf. on Control, Communication and Power Engineering 2010.

[13] Pinaki Mitra, Student Member, IEEE, and Ganesh Kumar Venayagamoorthy, Senior Member, IEEE, "An Adaptive Control Strategy for DSTATCOM Applications in an Electric Ship Power System", IEEE Transactions on Power Electronics, vol. 25, no. 1, January 2010.

[14] Mahesh K. Mishra, Member, IEEE, and K. Karthikeyan, "A Fast-Acting DC-Link Voltage Controller for Three-Phase DSTATCOM to Compensate AC and DC Loads", IEEE Transactions on Power Delivery, vol. 24, no. 4, October 2009.

[15] Chandan Kumar and Mahesh K. Mishra, "A Modified DSTATCOM Topology with Reduced VSI Rating, DC Link Voltage, and Filter Size", Clean Electrical Power (ICCEP), 2013 International Conference on DOI: 10.1109/ICCEP.2013.6587009, Publication Year: 2013, Page(s): 325 – 331.

[16] Srinivas Bhaskar Karanki, Nagesh Geddada,Mahesh K. Mishra and B. Kalyan Kumar, "A DSTATCOM Topology With Reduced DC-Link Voltage Rating for Load Compensation with Nonstiff Source", IEEE Transactions on Power Electronics, vol. 27, no. 3, March 2012.

[17] Mahesh K. Mishra and K. Karthikeyan, "An investigation on design and switching dynamics of a voltage source inverter to compensate unbalanced and nonlinear loads," IEEE Trans. Ind. Electron., vol. 56, no. 8, pp. 2802–2810, Aug. 2009.

[18] George Adam, Alina Georgiana Stan (Baciu), Gheorghe Livinţ, "An Adaptive Hysteresis Band Current Control For Three Phase Shunt Active Power Filter Using Fuzzy Logic", 2012 International Conference and Exposition on Electrical and Power Engineering (EPE 2012), 25-27 October, Iasi, Romania.

[19] Mr.Y.Prakash and Dr. S.Sankar," Power Quality Improvement Using DVR in Power System", 2014 Power and Energy Systems: Towards Sustainable Energy (PESTSE 2014).

[20] V. Khadkikar, A. Chandra, A. O. Barry and T. D. Nguyen , "Conceptual Study of Unified Power Quality Conditioner (UPQC)", IEEE ISIE, July 9-12, 2006, Montreal, Quebec, Canada.

[21] Bharath Babu Ambati and Vinod Khadkikar, "Optimal Sizing of UPQC Considering VA Loading and Maximum Utilization of Power-Electronic Converters", IEEE Transactions on Power Delivery, vol. 29, no. 3, June 2014.

[22] Hirofumi Akagi, Edson Hirokazu Watanabe and Mauricio Aredes "Instantaneius power theory and applications to power conditioning" IEEE-press chapter 3-4, 2007.

[23] Karuppanan P. and Kamala Kanta Mahapatra, "A Novel Control Strategy based Shunt APLC for Power Quality Improvements", Power, Control and Embedded Systems (ICPCES), 2010.

[24] C.N. Rowey, T.J. Summersz, R.E. Betz and D. Cornforth, "A Comparison of Instantaneous and Fryze Power Calculations on P-F and Q-V Droop in Microgrids", Universities Power Engineering Conference (AUPEC), 2010.

[25] Mauricio Aredes and Luis F. C. Monteiro, "A Control Strategy for Shunt Active Filter", Harmonics and Quality of Power, 10th International Conference on 6-9 Oct. 2002.

[26] Alexandru Bitoleanu and Mihaela Popescu, "Shunt Active Power Filter; Overview on the Reference Current Methods Calculation and their Implementation", 4th International Symposium Electrical and Electronics Engineering (ISEEE), 2013.

[27] Bhim Singh, Sunil Kumar Dube, Sabha Raj Arya, Ambrish Chandra and Kamal Al-Haddad, "A Comparative Study of Adaptive Control Algorithms in Distribution Static Compensator", Industrial Electronics Society, 39th Annual Conference of the IEEE DOI: 10.1109/IECON.2013.6699126, Publication Year: 2013 , pp. 145 – 150.

[28] Maryclaire Peterson, Brij N. Singh and Parviz Rastgoufard, "Active and Passive Filtering for Harmonic Compensation", 40th Southeastern Symposium on System Theory MC1.5 University of New Orleans New Orleans, LA, USA, March 16-18, 2008.

[29] Alexander D. Poularikas and Zayed M. Ramadan, "Adaptive Filtering Primer with MATLAB", 2006 by Taylor & Francis Group, LLC.

[30] Simon S. Haykin, "Adaptive Filter Theory", Prentice Hall, 2001, 4th Edition.

[31] Bhim Singh And Jitendra Solanki, "An Implementation Of An Adaptive Control Algorithm For A Three-Phase Shunt Active Filter" IEEE Trans. on Industrial Electronics, Vol. 56, No. 8, August 2009.

[32] Djaffar Ould Abdeslam, Patrice Wira, Jean Mercklé, Damien Flieller, and Yves-André Chapuis, "A Unified Artificial Neural Network Architecture for Active Power Filters", IEEE Transactions on Industrial Electronics, vol. 54, no. 1, February 2007.

[33] Sireesha N., K. Chithra and Tata Sudhakar, "Adaptive filtering based on Least Mean Square Algorithm", Ocean Electronics (SYMPOL), IEEE Conference Publications, Publication Year: 2013 , pp. 42 – 48.

[34] Bhim Singh, Sabha Raj Arya, Ambrish Chandra and Kamal Al-Haddad, "Implementation of Adaptive Filter in Distribution Static Compensator", IEEE Transactions on Industry Applications, 10.1109/TIA.2014.2304623.

[35] P. Wira, D. Ould Abdeyslam and J. Mercklé, "Learning and adaptive techniques for harmonics compensation in power supply networks", 978-1-4244-1633-2/08/2008 IEEE.

[36] Paulo S.R. Diniz. "Nonlinear Adaptive Filtering", Adaptive Filtering, 2008.

[37] Dhull, Sanjeev Kumar, Arya, Sandeep K. and Sahu, "Performance Comparison of Adaptive Algorithms for Adaptive line Enhancer", International Journal of Computer Science Issues (IJCSI), 2011.

[38] Javier Garcia-Casado. "Adaptive filtering of ECG interference on surface EEnGs based on signal averaging", Physiological Measurement, 06/01/2006.

[39] Grimble, "Adaptive Finite Impulse Response Filters", Advanced Textbook in Control and Signal Processing, 2005.

[40] Farzad Nekouei, Neda Zargar Talebi, Yousef S. Kavian, and Ali Mahani. "FPGA implementation of LMS self-correcting adaptive filter (SCAF) and hardware analysis", 8th International Symposium on Communication Systems Networks & Digital Signal Processing (CSNDSP), 2012.

[41] Leonardo S. Resende, João Marcos T. Romano, and Maurice G. Bellanger,“Split Wiener Filtering With Application in Adaptive Systems”, IEEE Transactions on Signal Processing, vol. 52, no. 3, pp. 636-644, March 2004.

[42] Devi, T. Meera, Kasthuri, N. and Natarajan, A. M., "Environmental Noise Classification and Cancellation using Fuzzy Classifier and Fuzzy Adaptive Filters", International Journal of Computer Science Issues (IJCSI), 2012.

[43] Moreau, "Feed-forward Control System Design", Active Control of Noise and Vibration Second Edition, 2012.

[44] Paulo S.R. Diniz. "The Least-Mean-Square (LMS) Algorithm", Adaptive Filtering, 2008.

[45] Badong Chen', Jinchun Hu, Hongbo Li and Zengqi Sun, "Adaptive filtering under maximum mutual information criterion", Neuro-computing, Brazilian Symposium on Neural Networks, Volume 71, Issues 16–18, October 2008, pp. 3680–3684.

[46] Tülay Adali and Simon Haykin, “Adaptive Signal Processing: Next Generation Solutions”, John Wiley & Sons, 2006.

[47] Sabha Raj Arya and Bhim Singh, “Performance of DSTATCOM Using Leaky LMS Control Algorithm”, IEEE Journal of emerging and selected topics in Power Electronics, vol. 1, no. 2, June 2013.

APPENDIX

Parameters of the proposed distribution network system in simulations and hardware:

Sl. No.	Parameters	Value
1	Line to line rms source voltage	110V
2	System frequency (f)	50 Hz
3	Source impedances	$R_s = 0.15\ \Omega$
		$L_s = 0.5$ mH
4	Interfacing Filter impedance	$R_c = 0.2\ \Omega$, $L_c = 3.2$ mH,
5	3-phase diode rectifier load	R = 18-60 Ω
		L = 100 mH
6	Capacitance of DC link capacitor	1650 μF

PUBLICATIONS

Published

[1] Sachin Kumar Kesharvani, Alka Singh and Manoj Badoni, "'Conductance based Fryze Algorithm for Improving Power Quality for Non-linear Loads", in International Conference on Signal Propagation and Computer Technology (ICSPCT)-2014 at Govt. Engineering College Ajmer, India, Technical Sponsored by IEEE Delhi Section.